Reactions of Diynes on the M_3P Cluster Face of $Ru_4(CO)_{13}(\mu_3$-PPh): Alkyne Coordination, Phosphorus–Carbon Coupling, and Skeletal Rearrangement. X-ray Structures of *nido*-$Ru_4(CO)_{10}(\mu$-CO)$_2\{\mu_4$-η^1,η^1,η^2-P(Ph)C(C≡CMe)CMe$\}$, *closo*-$Ru_4(CO)_{10}(\mu$-CO)$(\mu_4$-PPh$)\{\mu_4$-$\eta^1,\eta^1,\eta^2,\eta^2$-(RC≡C)C≡CR$\}$ (R = Ph, Me), and $Ru_4(CO)_{10}(\mu_4$-PPh$)(\mu_4$-$\eta^1,\eta^1,\eta^3,\eta^3$-$SiMe_3C_4SiMe_3)$

John F. Corrigan, Simon Doherty, Nicholas J. Taylor, and Arthur J. Carty*

Guelph-Waterloo Centre for Graduate Work in Chemistry, Waterloo Campus, Department of Chemistry, University of Waterloo, Waterloo, Ontario, Canada N2L 3G1

Received September 11, 1992

Reaction of the butterfly cluster *nido*-$Ru_4(CO)_{13}(\mu_3$-PPh) (1) with 1,3-diynes RC≡CC≡CR (R = Ph, Me, $SiMe_3$) occurs under thermal conditions affording, as the first-formed products, the 62-electron clusters *nido*-$Ru_4(CO)_{10}(\mu$-CO$)_2\{\mu_4$-η^1,η^1,η^2-P(Ph)C(C≡CR)CR$\}$ (R = Ph, **2a**; R = $SiMe_3$, **2b**; R = Me, **2c**). Formation of **2a–c** involves facile P–C bond formation retaining the 62-cluster valence electron count (CVE) associated with the butterfly skeletal framework. Coordination of a single acetylenic triple bond of the 1,3-diyne fragment in **2a–c** affords an overall six electron donor P(Ph)C(C≡CR)CR fragment. A single-crystal X-ray structure determination of **2c** was carried out: **2c** crystallizes as monoclinic crystals, space group $P2_1/n$ with unit cell dimensions a = 9.800(2) Å, b = 25.364(7) Å, c = 12.722(4) Å, β = 98.50(2)°, V = 3127.6(15) Å^3, and Z = 4. The structure was solved and refined to R and R_w values of 0.0235 and 0.0337, respectively, on the basis of 4670 observed ($F \geq 6.0\sigma(F)$) data. The structure of **2c** revealed that the acetylene was bonded in a μ_3–η^2-manner to the Ru_2P open triangle of the Ru_3P square base reinforcing the view that the phosphinidene fragment behaves as an integral part of the skeletal framework. These addition reactions have been spectroscopically shown to proceed with high regiospecificity. Clusters **2a–c** undergo a facile skeletal transformation concomitant with loss of a single carbon monoxide molecule to afford the 62-electron clusters *closo*-$Ru_4(CO)_{10}(\mu$-CO$)(\mu_4$-PPh$)\{\mu_4$-$\eta^1,\eta^1,\eta^2,\eta^2$-(RC≡C)C≡CR$\}$(R = Ph, **3a**; R = $SiMe_3$, **3b**; R = Me, **3c**). This skeletal rearrangement involves P–C bond cleavage and transfer of the μ_3-PPh vertex originally basal to an apical position, adopting its more familiar role as a μ_4-cluster stabilizing fragment. We determined that the transformations **2a** to **3a** and **2c** to **3c** occurred with opposite regiochemistry of rearrangement, a feature confirmed via single-crystal X-ray structures of both **3a** and **3c**. Crystals of **3a** are triclinic, space group $P\bar{1}$, a = 9.255(1) Å, b = 9.677(1) Å, c = 20.531(2) Å, α = 80.47(1)°, β = 79.72(1)°, γ = 75.84(1)°, V = 1739.9(3) Å^3, and Z = 2; for **3c**, monoclinic, space group Cc, a = 11.873(2) Å, b = 14.974(2) Å, c = 16.293(3) Å, β = 106.15(1)°, V = 2782.1(8) Å^3, and Z = 4. The structures were solved and refined to the following R and R_w values: **3a**, R = 0.0291 and R_w = 0.0459 on 6565 observed ($F \geq 6.0\sigma(F)$) data; **3c**, R = 0.0203 and R_w = 0.0255 on 3112 observed ($F \geq 6.0\sigma(F)$) data. The cluster core geometries of **3a–c** are based on a closo pentagonal bipyramidal arrangement of Ru_4PC_2 atoms, consistent with current bonding theories (eight skeletal electron pairs, seven vertices). Of clusters **3a–c** only **3a** and **3b** undergo further thermal transformation. These clusters decarbonylate smoothly to form the decacarbonyl clusters $Ru_4(CO)_{10}(\mu_4$-PPh$)(\mu_4$-$\eta^1,\eta^1,\eta^3,\eta^3$-RC≡CC≡CR) (R = Ph, **4a**; R = $SiMe_3$, **4b**) in reasonable yields. A single-crystal X-ray structure determination of **4b** revealed a square planar arrangement of metal atoms on which both acetylenic multiple bonds were coordinated, affording a novel 8e donor four carbon hydrocarbyl ligand for which a bis-μ_3-(alkylidyne) dicarbide description is appropriate. A cluster electron count of 64 electrons is in accord with the effective atomic number rule and the presence of four M–M bonds. Crystals of **4b** are orthorhombic, space group *Pnma*, a = 21.727(3) Å, b = 13.954(2) Å, c = 11.462(1) Å, V = 3475.0(8) Å^3, and Z = 4. The structure was solved and refined to R = 0.0299 and R_w = 0.0334 on 3979 observed ($F \geq 6.0\sigma(F)$) data. Cluster **2a** reacts with dihydrogen thermally (90°C n-heptane 60 min, 4 mol equiv) resulting in elimination of the corresponding trans monoene and formation of the known cluster $H_2Ru_4(CO)_{12}(\mu_3$-PPh) **5**.

Introduction

The butterfly cluster framework has attracted considerable interest in recent years,[1] a direct consequence of both its structural and electronic versatility.[2] This has recently inspired intense theoretical and structural investigations.[3] Novel reactivity patterns have been ex-

0276-7333/93/2312-1365$04.00/0

hibited by butterfly clusters with nonclassical electron counts and geometries.[4] There exist many examples of butterfly clusters containing small molecules (acetylenes,[5] phosphinidenes,[6] mercaptides,[7] alkylidynes,[8] azoalkanes[9])- or bare main group atoms (N,[10] C[11]) coordinated within the cavity between the wingtip atoms. The chemistry of clusters exhibiting these structural characteristics represents a significant research area, a result of the unusual reactivity patterns that this flexible coordination environment confers upon these ligands. Moreover, clusters in this category have been shown to facilitate activation of small molecules.[12] However in many such instances the coordinated main group ligand appears to adopt a passive role, probably acting to retain the cluster nuclearity. In the case where main group atoms direct or enhance reactivity, factors influencing the mode of reaction are poorly understood. The butterfly skeletal framework of metal atoms also possesses the capacity to serve as a model for the chemisorption of small unsaturated hydrocarbons or for C–X bond-forming/cleavage processes occurring at a catalytically active step in a metal (or alloy) surface.[1,13]

The unusual reactivity of stabilized naked main group atoms bound in either μ_4, μ_3, or μ_2 fashion between the wingtip metal atoms of a butterfly cluster has been widely investigated and continues to be of interest as do the electronic and steric properties that govern reactivity patterns. Yet there are few reports relating to the role and activating influence of main group elements as skeletal atoms in such clusters.[14] Incorporating main group vertices into a cluster framework should produce a pronounced effect on cluster reactivity and should be reflected in subsequent ligand transformations and skeletal rearrangements. Recently, we have shown that cluster 1 undergoes a facile P–C bond forming reaction with diphenylacetylene,[15] the product undergoing a further transformation to $Ru_4(CO)_{10}(\mu\text{-}CO)(\mu_4\text{-}PPh)(\mu_4\text{-}\eta^1,\eta^1,\eta^2,\eta^2\text{-}PhC{\equiv}CPh)$. This process demonstrates the ability of a μ_3-phosphinidene fragment "PPh" to be considered as an integral part of the skeletal framework. The capping sulfido ligand in the 60e tetrahedral cluster $Os_4(CO)_{12}(\mu_3\text{-}S)$ has similarly been shown to undergo S–C bond-forming reactions with functionalized acetylenes[14a] as have μ-imido[16] and several other ligand bridged clusters,[17,18] revealing a tendency for incoming acetylenic ligands to engage in an initial interaction with the main-group bridging ligand prior to further ligand transformations.[17]

The shortcomings of bridging or capping main group atoms as cluster stabilizing entities has long been established.[16,18-20] However, these main-group fragments are valuable not only for their influence toward incoming ligands but also for their capacity to participate in skeletal rearrangements while maintaining the cluster nuclearity. The tendency of these clusters to take part in such reactions has been attributed to the comparable enthalpies of the M–M and M–P bonds, and in the absence of a vacant coordination site or a favourable reaction center, competing reactions are often observed.[21] The development of useful chemistry for phosphido- and phosphinidene-stabilized clusters relies on the presence of either a reactive ligand susceptible to attack by incoming reagents[22a] or an activated cluster framework.[22b]

Attempts to incorporate alkynes into the medium-nuclearity clusters has often led to the isolation of various products in low yields,[23] a consequence of the forcing conditions required for reaction to occur. Those reactions that proceed with high yields of product usually employ lightly stabilized or activated clusters. Compound 1 provides a unique opportunity to study such reactions

(1) Sappa, E.; Tiripicchio, A.; Carty, A. J.; Toogood, G. E. *Prog. Inorg. Chem.* **1987**, *35*, 437.
(2) Carty, A. J.; MacLaughlin, S. A.; Van Wagner, J.; Taylor, N. J. *Organometallics* **1982**, *1*, 1013. (b) Churchill, M. R.; Bueno, C.; Young, D. A. *J. Organomet. Chem.* **1981**, *213*, 139. (c) Hogarth, G.; Phillips, J. A.; van Gastel, F.; Taylor, N. J.; Marder, T. B.; Carty, A. J. *J. Chem. Soc., Chem. Commun.* **1988**, 1570.
(3) Osella, D.; Ravera, M.; Nervi, C.; Housecroft, C. E.; Raithby, P. R.; Zanello, P.; Laschi, F. *Organometallics* **1991**, *10*, 3253.
(4) (a) Adams, R. D.; Yang, L. W. *J. Am. Chem. Soc.* **1982**, *104*, 4115. (b) Adams, R. D.; Yang, L. W. *J. Am. Chem. Soc.* **1983**, *105*, 234.
(5) (a) Dahl, L. F.; Smith, D. L. *J. Am. Chem. Soc.* **1962**, *84*, 2450. (b) Gervasio, G.; Rossetti, R.; Stanghellini, P. L. *Organometallics* **1985**, *4*, 1612. (c) Rumin, R.; Robin, F.; Petillon, F. Y.; Muir, K. W.; Stevenson, I. *Organometallics* **1991**, *10*, 2274. (d) Sappa, E.; Belletti, D.; Tiripicchio, A.; Tiripicchio-Camellini, M. *J. Organomet. Chem.* **1989**, *359*, 419. (e) Lentz, D.; Micheal, H. *Angew. Chem.*, Int. Ed. *Eng.* **1988**, *100*, 871. (f) Albiez, T.; Powell, A. K.; Vahrenkamp, H. *Chem. Ber.* **1990**, *123*, 667. (g) Bantel, H.; Powell, A. K.; Vahrenkamp, H. *Chem. Ber.* **1990**, *123*, 661.
(6) MacLaughlin, S. A.; Carty, A. J.; Taylor, N. J. *Can. J. Chem.* **1982**, *60*, 87.
(7) Rossi, S.; Pursiainen, J.; Pakkanen, T. A. *Organometallics* **1991**, *10*, 1390.
(8) (a) Tachikawa, M.; Muetterties, E. L. *J. Am. Chem. Soc.* **1980**, *102*, 4541. (b) Beno, M. A.; Williams, J. M.; Tachikawa, M.; Muetterties, E. L. *J. Am. Chem. Soc.* **1980**, *102*, 4542.
(9) Bantel, H.; Hansert, B.; Powell, A. K.; Tasi, M.; Vahrenkamp, H. *Angew. Chem., Int. Ed. Engl.* **1989**, *28*, 1059.
(10) Collins, M. A.; Johnson, B. F. G.; Lewis, L.; Mace, J. M.; Morris, J.; McPartlin, M.; Nelson, W. J. H.; Puga, J.; Raithby, P. R. *J. Chem. Soc., Chem. Commun.* **1983**, *689*. (b) Blohm, M. L.; Gladfelter, W. L. *Organometallics* **1985**, *4*, 45.
(11) (a) Cowie, A. G.; Johnson, B. F. G.; Lewis, J.; Raithby, P. R. *J. Organomet. Chem.* **1988**, *306*, C63. (b) Holt, E. M.; Whitmire, K. H.; Shriver, D. F. *J. Organomet. Chem.* **1981**, *213*, 125. (c) Adams, R. D.; Babin, J. E.; Tanner, J. T. *Organometallics* **1988**, *7*, 765.
(12) van Gastel, F.; Corrigan, J. F.; Doherty, S.; Taylor, N., J.; Carty, A. J. *Inorg. Chem.* **1992**, *31*, 4492.
(13) (a) Muetterties, E. L.; Rhodes, T. N.; Band, E.; Brucker, C. F.; Pretzer, W. R. *Chem. Rev.* **1979**, *79*, 91.
(14) (a) Adams, R. D.; Wang, S. *Organometallics* **1985**, *4*, 1902. (b) Adams, R. D.; Wang, S. *J. Am. Chem. Soc.* **1987**, *109*, 924. (c) Hansert, B.; Powell, A. K.; Vahrenkamp, H. *Chem. Ber.* **1991**, *124*, 2697. (d) Knoll, K.; Fassler, T.; Huttner, G. *J. Organomet. Chem.* **1987**, *332*, 309. (e) Eber, B.; Buchholz, D.; Huttner, G.; Fassler, T.; Imhof, W.; Fritz, M.; Daran, J. C.; Jeannin, Y. *J. Organomet. Chem.* **1991**, *401*, 49.
(15) Lunniss, J.; MacLaughlin, S. A.; Taylor, N. J.; Carty, A. J.; Sappa, E. *Organometallics* **1985**, *4*, 2066.
(16) Song, J. S.; Han, S. H.; Nguyen, S. T.; Geoffroy, G. L.; Rheingold, A. L. *Organometallics* **1990**, *9*, 2386. (b) Song, J. S.; Geoffroy, G. L.; Rheingold, A. L. *Inorg. Chem.* **1992**, *31*, 1505.
(17) (a) Adams, R. D.; Wang, S. *Organometallics* **1987**, *6*, 739. (b) Adams, R. D.; Wang, S. *Organometallics* **1986**, *5*, 1274. (c) Rauchfuss, T. B.; Rodgers, D. P. S.; Wilson, S. R. *J. Am. Chem. Soc.* **1986**, *108*, 3114. (d) Rajan, O. A.; Mckenna, M.; Noordik, J.; Haltiwanger, R. C.; Rakowski DuBois, M. *Organometallics* **1983**, *3*, 831.
(18) (a) Knoll, K.; Huttner, G.; Fassler, T.; Zsolnai, L. *J. Organomet. Chem.* **1987**, *327*, 255. (b) Knoll, K.; Huttner, G.; Zsolnai, L.; Orama, O. *Angew. Chem., Int. Ed. Engl.* **1986**, *25*, 1119. (c) Knoll, K.; Orama, O.; Huttner, G. *Angew. Chem., Int. Ed. Engl.* **1984**, *23*, 976. (d) Huttner, G.; Knoll, K. *Angew. Chem., Int. Ed. Engl.* **1987**, *26*, 743.
(19) Adams, R. D.; Belinski, J. A. *Organometallics* **1991**, *10*, 2114.
(20) Haines, J. S.; Haines, R. J.; Smit, D. N.; Natarajan, K.; Scheidsteger, O.; Huttner, G. *J. Organomet. Chem.* **1982**, *240*, C23. (b) Jaeger, T.; Vahrenkamp, H. *Z. Naturforsch.* **1986**, *B41*, 789. (c) Nuel, D.; Dahan, F.; Mathieu, R. *Organometallics* **1986**, *5*, 1278. (d) Williams, G. D.; Geoffroy, G. L.; Whittle, R. R.; Rheingold, A. L. *J. Am. Chem. Soc.* **1985**, *107*, 729. (e) Williams, G. D. Whittle, R. R.; Geoffroy, G. L.; Rheingold, A. L. *J. Am. Chem. Soc.* **1987**, *109*, 3936.
(21) (a) Vahrenkamp, H. *Adv. Organomet. Chem.* **1983**, *22*, 169. (b) Vahrenkamp, H. *Angew. Chem., Int. Ed. Engl.* **1978**, *17*, 379. (c) Frieser, B. S. In *Bonding Energetics of Organometallic Compounds*; Marks, T. J., Eds.; ACS Symposium Series 428; American Chemical Society: Washington, DC, 1990; p 55.
(22) (a) Nucciarone, D.; MacLaughlin, S. A.; Taylor, N. J.; Carty, A. J. *Organometallics* **1988**, *7*, 106. (b) Fogg, D. F.; Carty, A. J. *Polyhedron* **1988**, *7*, 2285.
(23) (a) Raithby, P. R.; Rosales, M. J. *Adv. Inorg. Radiochem.* **1985**, *29*, 169. (b) Sappa, E.; Tiripicchio, A.; Braunstein, P. *Chem. Rev.* **1983**, *83*, 203. (c) Deeming, A. J. In *Transition Metal Clusters*; Johnson, B. F. G., Ed.; Wiley: Chichester, 1980; Chapter 6.

since alkyne incorporation occurs under mild conditions affording workable yields of a single major product. This convenient route into hydrocarbyl-substituted tetranuclear clusters is facilitated by the above-mentioned facile P–C coupling reaction followed by a skeletal transformation. The reaction of 1 with PhC≡CPh to yield $Ru_4(CO)_{10}(\mu$-$CO)_2\{\mu_4$-η^1,η^1,η^2-P(Ph)CPhCPh} (6) represents an example of such a process.[15] Loss of carbon monoxide from 6 and oxidative addition of the so-formed phosphorus–carbon bond affords the cluster *closo*-$Ru_4(CO)_{10}(\mu$-$CO)(\mu_4$-Ph)-$(\mu_4$-$\eta^1,\eta^1,\eta^2,\eta^2$-PhC≡CPh) (7). Extending our investigations to the reaction of 1 with 1,3 diynes resulted in a further unique skeletal transformation, requiring coordination of both acetylenic triple bonds to the square planar arrangement of ruthenium atoms and resulting in a rare coordination mode for the four-carbon hydrocarbyl bridging ligands.[24]

Experimental Section

General Procedures. Standard Schlenk techniques were used for all reactions, and manipulations were carried out under a dry dinitrogen atmosphere. All solvents were dried (hexane and tetrahydrofuran over sodium/benzophenone, heptane, and toluene over $LiAlH_4$ and methylene chloride over P_2O_5), deoxygenated, and distilled prior to use.

All reactions were monitored by thin-layer chromatography (Baker Flex, silica gel 1B-F). Purification of products was performed by column chromatography using silica gel (70–230 mesh) or by thin-layer chromatography using silica gel plates (20 cm × 20 cm, Merck, TLC grade, Aldrich Chemical Co.). Solution infrared spectra were recorded on a Nicolet-520 FTIR spectrometer using sodium chloride cells of path length 0.5 mm. NMR spectra were recorded on Bruker AM-250 or AC-200 instruments, and chemical shifts were referenced internally to the solvent $CDCl_3$ (^1H and $^{13}C\{^1H\}$) or externally to 85% H_3PO_4 ($^{31}P\{^1H\}$). Microanalyses were performed by M-H-W Laboratories, Phoenix, AZ.

Dodecacarbonyl triruthenium was purchased from Strem Chemical Co., diphenylphosphine from Aldrich Chemical Co., and diphenylbutadiyne, bis(trimethylsilyl)butadiyne, and 2,4-hexadiyne from Farchan Laboratories. These were used without further purification. The cluster $Ru_4(CO)_{13}(\mu_3$-PPh) (1) was prepared via the pyrolysis of $(\mu$-H)$Ru_3(CO)_9(\mu$-$PPh_2)$ as previously reported.[6]

Syntheses and Characterization. Preparation of $Ru_4(CO)_{10}(\mu$-CO$)_2\{\mu_4$-η^1,η^1,η^2-P(Ph)C(C≡CPh)CPh} (2a). To a solution of 1 (0.21 g, 0.24 mmol) in n-hexane (80 mL) was added 1,4-diphenylbutadiyne (0.24 g, 1.2 mmol). The reaction mixture was heated at 50 °C for 5 h during which time the reaction solution changed color from deep red to orange-brown. Monitoring the progress of the reaction by IR spectroscopy indicated the smooth conversion of 1 to $Ru_4(CO)_{10}(\mu$-$CO)_2\{\mu_4$-η^1,η^1,η^2-P(Ph)C(C≡CPh)-CPh} (2a) and $Ru_4(CO)_8(\mu_4$-PPh)[$\eta^1,\eta^1,\eta^2,\eta^2$-(Ph)CC(C≡CPh)C-(Ph)C-$\eta^4$-CC(Ph)C(Ph)C(C≡CPh)] (8). The solution was cooled to room temperature and the solvent removed under reduced pressure, yielding a brown oily residue. This residue was dissolved in the minimum of dichloromethane, absorbed onto silica gel, placed on a 200- × 10-mm silica gel column, and eluted with a hexane/dichloromethane (100:10, v/v) mixture to afford three well-separated bands. The first band eluted was characterized spectroscopically as 1 (0.020 g, 0.023 mmol, 9%). The following green-brown fraction was identified as **2a** (0.091 g, 0.09 mmol, 36%). The collected fraction was concentrated and left overnight at −20 °C affording brown crystals. The final band to elute gave after concentration and cooling at −20 °C orange crystals (0.13 g, 0.098 mmol, 41%) of $Ru_4(CO)_8(\mu_4$-PPh)[$\eta^1,\eta^1,\eta^2,\eta^2$-(Ph)CC-(C≡CPh)C(Ph)C-$\eta^4$-CC(Ph)C(Ph)C(C≡CPh)] (8) characterized by comparison of its spectroscopic properties with those previously reported.[25]

Data for **2a**. IR (ν(CO), cm^{-1} C_6H_{12}): 2087(m), 2056(s), 2045-(s), 2038(s), 2042(m), 2112(sh), 2008(w), 1987(w), 1983(w), 1979-(w), 1858(w), 1828(w). $^{31}P\{^1H\}$ NMR (101.3 MHz, $CDCl_3$, δ): 40.5 (s). $^{13}C\{^1H\}$ NMR (62.8 MHz, $CDCl_3$, δ): 207 (d, CO, $^2J_{PC}$ = 6.5 Hz), 198.4 (d, CO, $^2J_{PC}$ = 13.0 Hz), 192.7 (d, CO, $^2J_{PC}$ = 68.0 Hz), 186.7 (d, CO, $^2J_{PC}$ = 5.0 Hz), 185.2 (d, C acetylene, $^2J_{PC}$ = 30.0 Hz), 151.6 (d, C ipso, $^1J_{PC}$ = 18.0 Hz), 137.6 (d, C ipso, $^1J_{PC}$ = 35.0 Hz), 133.7 (d, C ortho, $^2J_{PC}$ = 11.0 Hz), 131.7 (s, C para), 128–129.2 (phenyl), 122.2 (s, C ipso), 92.0 (d, C acetylene, J_{PC} = 5.0 Hz), 91.5 (d, C acetylene, J_{PC} = 11.0 Hz), 89.0 (d, C acetylene, J_{PC} = 41.0 Hz). Anal. Calcd for $C_{34}H_{15}O_{12}PRu_4$: C, 38.88; H, 1.44. Found: C, 39.01; H, 1.53.

Preparation of $Ru_4(CO)_{10}(\mu$-$CO)_2\{\mu_4$-η^1,η^1,η^2-P(Ph)C(C≡C-Me)CMe} (2c) and $Ru_4(CO)_{10}(\mu$-$CO)_2\{\mu_4$-η^1,η^1,η^2-P(Ph)C-(C≡CSiMe$_3$)CSiMe$_3$} (2b). An n-hexane solution of $Ru_4(CO)_{13}$-$(\mu_3$-PPh) (1) (0.24 g, 0.27 mmol) was heated at 55–60 °C in the presence of a large excess of 2,4-hexadiyne (0.17 g, 2.2 mmol). After 3 h both thin-layer chromatography and IR spectroscopy showed that all the starting material had been consumed. The reaction solution was cooled and the solvent removed under reduced pressure to leave a brown oily residue. A chromatographic procedure similar to that employed for the purification of **2a** afforded two major products. The first well-separated band to elute was identified as **2c**. Concentration and subsequent cooling (−20 °C) of this fraction yielded deep brown crystals of **2c** (0.16 g, 0.17 mmol, 64%). A slower moving orange fraction, present in trace amounts only, was characterized as **3c** (vide infra). $Ru_4(CO)_{10}(\mu$-$CO)_2\{\mu_4$-η^1,η^1,η^2-P(Ph)C(C≡CSiMe$_3$)CSiMe$_3$} (**2b**) was prepared in a manner similar to the procedure described above for **2c** and isolated as brown crystals from dichloromethane/hexane (55%).

Data for **2b**. IR (ν(CO), cm^{-1}, C_6H_{12}): 2088(m), 2057(s), 2046-(s), 2038(s), 2023(m), 2016(w), 2007(w), 1992(w), 19873(w), 1858-(w), 1829(w). $^{31}P\{^1H\}$ NMR (101.3 MHz, $CDCl_3$, δ): 47.9 (s). ^1H NMR (250 MHz, CD_2Cl_2, δ): 7.28–7.32 (m, phenyl, 3 H), 7.1–7.2 (br, phenyl, 2 H), 0.19 (s, $SiMe_3$, 9 H), 0.06 (s, $SiMe_3$, 9 H). $^{13}C\{^1H\}$ NMR (62.8 MHz, CD_2Cl_2, δ): 205.0 (br, CO), 199.8 (d, CO, $^2J_{PC}$ = 14.8 Hz), 193.2 (d, CO, $^2J_{PC}$ = 66.0 Hz), 187.3 (d, CO, $^2J_{PC}$ = 4.6 Hz), 169.3 (d, C acetylene, J_{PC} = 22.1 Hz), 138.9 (d, C ipso, $^1J_{PC}$ = 30.0 Hz), 133.8 (d, C ortho, $^2J_{PC}$ = 12.3 Hz), 131.9 (s, C para), 128.6 (d, C meta, $^3J_{PC}$ = 10.8 Hz), 121.5 (s, C acetylene), 113.1 (d, C acetylene, J_{PC} = 37.4 Hz), 107.5 (s, C acetylene), 0.07 (s, $Si(CH_3)_3$, $^1J_{SiC}$ = 15.0 Hz), −0.6 (s, $Si(CH_3)_3$, $^1J_{SiC}$ = 15.4 Hz). Anal. Calcd for $C_{28}H_{23}O_{12}PRu_4Si_2$: C, 32.26; H, 2.22. Found: C, 32.44; H, 2.27.

2c. IR (ν(CO), cm^{-1}, C_6H_{12}): 2087(m), 2056(s), 2043(s), 2038-(s), 2023(w), 2014(w), 2004(w), 1990(w), 1980(w), 1859(w), 1832-(w). $^{31}P\{^1H\}$ NMR (101.3 MHz, $CDCl_3$, δ): 42.6 (s). ^1H NMR (250 MHz, CD_2Cl_2, δ): 7.35 (m, phenyl, 3 H), 7.1 (m, phenyl 2 H), 3.3 (d, CH_3, J_{PH} = 2.1 Hz, 3 H), 1.78 (d, CH_3, J_{PH} = 4.2 Hz, 3 H). $^{13}C\{^1H\}$ NMR (50.32 MHz, $CDCl_3$, δ): 205.0 (br, CO), 198.3 (d, CO, J_{PC} = 14.1 Hz), 192.5 (d, CO, $^2J_{PC}$ = 63.9 Hz), 186.5 (s, CO), 186.2 (d, C acetylene, J_{PC} = 21.6 Hz), 137.0 (d, C ipso, $^1J_{PC}$ = 33.7 Hz), 133.3 (d, C ortho, $^2J_{PC}$ = 11.3 Hz), 133.5 (s C para), 128.2 (d, C meta, $^3J_{PC}$ = 10.2 Hz), 90.8 (d, C acetylene, J_{PC} = 39.0 Hz), 90.7 (d, C acetylene, J_{PC} = 5.0 Hz), 79.7 (d, C acetylene, J_{PC} = 12.6 Hz), 38.1 (d, CH_3, $^2J_{PC}$ = 16.2 Hz), 4.27 (s, CH_3). Anal. Calcd for $C_{24}H_{11}O_{12}PRu_4$: C, 31.12; H, 1.20. Found: C, 31.20; H, 1.14.

Thermolysis of $Ru_4(CO)_{10}(\mu$-$CO)_2\{\mu_4$-η^1,η^1,η^2-P(Ph)C(C≡C-Ph)CPh} (2a). Heating an n-hexane solution (80 mL) of **2a** (0.14 g, 0.13 mmol) at reflux for 4 h resulted in a gradual color change from green-brown to deep orange. IR and TLC monitoring of the reaction indicated a smooth decarbonylation of **2a**. The solution was cooled to room temperature and the solvent removed under reduced pressure to leave an orange oily residue. The residue was extracted into dichloromethane and purified by

(24) Bobbie, B. J.; Taylor, N. J.; Carty, A. J. *J. Chem. Soc., Chem. Commun.* **1991**, 1511.

(25) Corrigan, J. F.; Doherty, S.; Taylor, N. J.; Carty, A. J. *Organometallics* **1992**, *11*, 3167.

chromatography on silica gel plates. Elution with hexane/CH_2Cl_2 (100:25 v/v) afforded a single major product identified as **3a**. Crystallization from CH_2Cl_2/hexane at −20 °C yielded deep orange crystals (0.09 g, 0.09 mmol, 66%). $Ru_4(CO)_{10}(\mu$-CO)$(\mu_4$-PPh)-$\{\mu_4$-$\eta^1,\eta^1,\eta^2,\eta^2$-(MeC≡C)C≡C(Me)$\}$ (**3c**) (60%) was prepared using a procedure similar to that described above with a marginally longer reaction time of 6 h.

3a. IR (ν(CO), cm^{-1}, C_6H_{12}): 2085(w), 2055(s), 2036(s), 2028(s), 2004(w), 1983(w), 1971(w), 1848(w). $^{31}P\{^1H\}$ NMR (101.3 MHz, $CDCl_3$, δ): 242.2 (s). ^1H (250 MHz, CD_2Cl_2, δ): 7.0–7.2 (m, phenyl, 9 H), 6.63 (d, phenyl, $^3J_{HH}$ = 6.7 Hz, 2 H), 6.56 (m, phenyl, 2 H), 6.25 (d, phenyl, $^3J_{HH}$ = 7.6 Hz, 2 H). $^{13}C\{^1H\}$ NMR (62.8 MHz, CD_2Cl_2, 298K, δ): 200.8 (d, CO, $^2J_{PC}$ = 12.6 Hz), 146.3 (s, C acetylene), 145.8 (s, C ipso), 133.3 (d, C ipso, $^1J_{PC}$ = 30.0 Hz), 125.3–131.8 (phenyl), 124.4 (s, C acetylene), 121.8 (s, C ipso), 99.1 (s, C acetylene), 92.7 (d, C acetylene, J_{PC} = 5.0 Hz). Anal. Calcd for $C_{33}H_{15}O_{11}PRu_4$: C, 38.77; H, 1.48. Found: C, 38.75, H, 1.69.

3c. IR (ν(CO), cm^{-1}, C_6H_{12}): 2084(w), 2054(s), 2035(s), 2030(s,sh), 2020(w), 2003(w), 1984(w), 1855(w). $^{31}P\{^1H\}$ NMR (101.3 MHz, CD_2Cl_2, δ): 242.0 (s). ^1H NMR (200 MHz, CD_2Cl_2, δ) 7.1–7.2 (m, phenyl, 3 H), 6.4–6.50 (m, H ortho, 2 H), 2.2 (s, CH_3, 3 H), 1.8 (s, CH_3, 3 H). $^{13}C\{^1H\}$ NMR (50.32 MHz, $CDCl_3$, δ): 201.6 (d, CO, $^2J_{PC}$ = 11.1 Hz), 173.1 (s, C acetylene), 133.3 (d, C ipso, $^1J_{PC}$ = 31.2 Hz), 130.5 (d, C para, $^4J_{PC}$ = 3.1 Hz) 129.9 (d, C ortho, $^2J_{PC}$ = 13.1 Hz), 129.4 (d, C meta, $^3J_{PC}$ = 12.6 Hz), 91.3 (s, C acetylene), 82.5 (s, C acetylene), 82.4 (s, C acetylene), 37.5 (s, CH_3), 4.2 (s, CH_3). Anal. Calcd for $C_{23}H_{11}O_{11}PRu_4$: C, 30.75; H, 1.23. Found: C, 31.00; H, 1.03.

Thermolysis of $Ru_4(CO)_{10}(\mu$-CO)$(\mu_4$-PPh$\{\mu_4$-$\eta^1,\eta^1,\eta^2,\eta^2$-(PhC≡C)C≡C(Ph)$\}$ (3a). A toluene solution (100 mL) of **3a** (0.14 g, 0.14 mmol) maintained at 100 °C for 7–8 h underwent a color change from deep orange to red orange. Monitoring the reaction solution by IR spectroscopy indicated formation of **4a**. The solution was cooled to room temperature and the solvent removed leaving an oily residue which was subsequently extracted into dichloromethane. This extract was absorbed onto silica gel and purified by column chromatography. Elution with a hexane/CH_2Cl_2 (75:25, v/v) mixture afforded a single major band. Concentration of the collected fraction and subsequent cooling to −20 °C afforded a 59% isolated yield of $Ru_4(CO)_{10}(\mu_4$-PPh)-$(\mu_4$-$\eta^1,\eta^1,\eta^2,\eta^2$-PhC≡CC≡CPh) (**4a**) as deep orange crystals (0.08 g, 0.08 mmol).

$Ru_4(CO)_{10}(\mu_4$-PPh$)(\mu_4$-$\eta^1,\eta^1,\eta^2,\eta^2$-$Me_3SiC{\equiv}CC{\equiv}CSiMe_3$) (**4b**) was prepared directly from **2b** using a procedure similar to that outlined above for the preparation of **4a**. Thermolysis was carried out at 97 °C in n-heptane, and concentration of the reaction mixture and storage at −20 °C overnight afforded orange crystals of **4b** in high yield (93%).

Data for **4a**. IR (ν(CO), cm^{-1}, CH_2Cl_2): 2083(w), 2059(s), 2027(m), 2020(m), 1966(w). $^{31}P\{^1H\}$ NMR (101.3 MHz, $CDCl_3$, δ): 442.2 (s). $^{13}C\{^1H\}$ NMR (50.3 MHz, CD_2Cl_2, δ): 203.8 (d, C acetylene, J_{PC} = 3.5 Hz), 194.7 (d, CO, J_{PC} = 9.0 Hz), 192.9 (d, C acetylene, J_{PC} = 38.7 Hz), 146.4 (s, C ipso), 142.5 (d, C ipso, $^1J_{PC}$ = 22.1 Hz), 139.3 (s, C ipso), 133.6–125.9 (phenyl), 111.5 (s, C acetylene), 74.3 (s, C acetylene). Anal. Calcd for $C_{32}H_{15}O_{10}PRu_4$: C, 38.64; H, 1.52. Found: C, 38.58; H, 1.44.

4b. IR (ν(CO), cm^{-1}, C_6H_{12}): 2080(w), 2056(s), 2025(m), 2015(m), 2005(w), 1966(w). $^{31}P\{^1H\}$ NMR (101.3 MHz, $CDCl_3$, δ): 451.8(s). ^1H NMR (250 MHz, CD_2Cl_2, δ): 7.55–7.1 (m, phenyl, 5 H), 0.63 (s, $SiMe_3$, 9 H), 0.14 (s, $SiMe_3$, 9 H). $^{13}C\{^1H\}$ NMR (62.8 MHz, CD_2Cl_2, δ): 204.8 (d, C acetylene, J_{PC} = 6.9 Hz), 194.7 (d, CO, J_{PC} = 9.5 Hz), 192.7 (d, C acetylene, J_{PC} = 38.9 Hz), 143.0 (d, C ipso, $^1J_{PC}$ = 22.2 Hz), 133.5 (d, C ortho, $^2J_{PC}$ = 13.1 Hz), 132.3 (s, C para), 128.3 (d, C meta, $^3J_{PC}$ = 11.5 Hz), 81.1 (d, C acetylene, J_{PC} = 6.6 Hz), 2.1 (s, $Si(CH_3)_3$), 0.9 (s, $Si(CH_3)_3$). Anal. Calcd for $C_{26}H_{23}O_{10}PRu_4Si_2$: C, 31.66; H, 2.35. Found: C, 31.86; H, 2.46.

Hydrogenation of $Ru_4(CO)_{10}(\mu$-CO$)_2\{\mu_4$-η^1,η^1,η^2-P(Ph)C-(C≡CPh)CPh$\}$ (2a). An n-heptane solution (100 mL) of **2a** (0.108 g, 0.1 mmol) purged with dihydrogen was heated at 90 °C for 60 min. A color change from green-brown to yellow was observed, completion of reaction being indicated by IR spectroscopy. The solvent was removed under reduced pressure and the residue extracted into dichloromethane. The extract was purified by chromatography on silica gel plates eluting with n-hexane/CH_2Cl_2 (110:10, v/v). The two major yellow products eluted were collected and identified as $H_2Ru_4(CO)_{12}(\mu_3$-PPh) **12** and $H_2Ru_3(CO)_9(\mu_3$-PPh).[26] A slower moving colorless band was collected, purified by GC, and characterized as *trans*-1,4-diphenylbut-1-ene.

X-ray Structure Analyses of 2c, 3a, 3c, and 4b. Brown crystals of **2c** were grown from a benzene/heptane solution at −20 °C. Crystals of **3a** and **4b** were obtained from dichloromethane/hexane solution at −20 °C, and crystals of **3c** were grown by the slow evaporation of a dichloromethane/methanol solution at room temperature. Suitable crystals were glued to glass fibers with epoxy resin and mounted on a goniometer head. Unit cell parameters were obtained, for all crystals, from least-squares refinements, of the setting angles for 25 reflections ($22 \le 2\theta \le 32°$) well dispersed in reciprocal space.

Collection and Reduction of X-ray Data. Details of the intensity data collection are given in Table I. Intensities for **2c**, **3a**, **3c**, and **4b** were all collected at room temperature using Mo Kα (λ = 0.710 73 Å) radiation and the ω scan method with a variable scan rate. Background measurements using the stationary crystal, stationary counter method were made at the beginning and end of each scan, each for 25% of the total scan time. Two standard reflections monitored every 100 reflections showed no significant changes during the data collection. Measured reflections were flagged as unobserved when ($F < 6.0\sigma(F)$) where σ was derived from counting statistics.

Solution and Refinement of the Intensity Data. Patterson syntheses readily yielded the positions of the four metal atoms in all cases, and standard Fourier methods were used to locate the remaining atoms in the molecules. This was followed by full-matrix least-squares refinement of positional and thermal parameters and subsequent conversion to anisotropic coefficients for all non-hydrogen atoms. At this stage for each structure a difference Fourier map revealed the positions of all hydrogen atoms. In subsequent refinements to convergence, hydrogen atom positions were located and fixed as riding on their respective carbon atoms with refined isotropic temperature coefficients. The function minimized in the least-squares calculations was $\sum w(|F_o| - |F_c|)^2$. The weighted R value is defined as $R_w = [\sum w(|F_o| - |F_c|)^2 / \sum w|F_o|^2]^{1/2}$ where the weights, w, are optimized on moderate intensities. Absorption corrections for **2c**, **3a**, and **3c** were applied using the face-indexed numerical procedure, and a semiempirical absorption correction was applied to **4b** based on a series of ψ scans. The atomic scattering factors used including anomalous dispersion corrections for ruthenium were taken from the *International Tables for X-ray Crystallography*;[27a] for hydrogen, those of Stewart et al. were used.[27b] All calculations were performed on a Microvax II and Vax 3000 using SHELXTL PLUS software. The final R and R_w values together with the residual electron density levels are given in Table I.

Compound **3c** crystallized in the noncentrosymmetric monoclinic space group *Cc*. The Friedel opposites in the range $0 \le h \le 15$, $0 \le k \le 19$, and $-21 \le l \le 20$ were collected. We found that the correct enantiomorph (absolute structure) was indeterminate from the merged data; however, using the unmerged Friedel pairs (6176 observed), the model presented here gave R and R_w values of 0.0293 and 0.0364, respectively. The alternative enantiomorph gave 0.0307 and 0.0386 for R and R_w.

Atomic positional parameters for **2c**, **3a**, **3c**, and **4b** are listed in Tables II, IV, VI, VIII respectively. Tables III, V, VII and IX contain appropriate selections of bond lengths and angles for these molecules.

(26) Iwasaki, F.; Mays, M. J.; Raithby, P. R.; Taylor, P. L.; Wheatley, P. J. *J. Organomet. Chem.* **1981**, *213*, 185.

(27) (a) *International Tables for X-ray Crystallography*; Kynoch Press: Birmingham, England, 1974; Vol. 4. (b) Stewart, R. F.; Davidson, E. R.; Simpson, W. T. *J. Chem. Phys.* **1965**, *42*, 3175.

Table I. Crystal and Intensity Data for $Ru_4(CO)_{10}(\mu\text{-}CO)_2\{\mu_4\text{-}\eta^1,\eta^1,\eta^2\text{-}P(Ph)C(C{\equiv}CMe)CMe\}$ (2c), $Ru_4(CO)_{10}(\mu\text{-}CO)(\mu_4\text{-}PPh)\{\mu^4\text{-}\eta^1,\eta^1,\eta^2,\eta^2\text{-}(RC{\equiv}C)C{\equiv}CR\}$ (R = Ph, 3a; R = Me, 3c), and $Ru_4(CO)_{10}(\mu_4\text{-}PPh)(\mu_4\text{-}\eta^1,\eta^1,\eta_3,\eta^3\text{-}SiMe_3C_4SiMe_3)$ (4b)

compd	2c	3a	3c	4b
formula	$C_{24}H_{11}O_{12}PRu_4{\cdot}0.5C_6H_6$	$C_{33}H_{15}O_{11}PRu_4$	$C_{23}H_{11}O_{11}PRu_4$	$C_{26}H_{23}O_{10}PRu_4Si_2$
molec wt	965.6	1022.7	898.6	986.9
cryst class	monoclinic	triclinic	monoclinic	orthorhombic
space group	$P2_1/n$	$P\bar{1}$	Cc	$Pnma$
a (Å)	9.800(2)	9.255(1)	11.873(1)	21.727(3)
b (Å)	25.364(7)	9.677(1)	14.974(2)	13.954(2)
c (Å)	12.722(4)	20.531(2)	16.293(3)	11.462(1)
α (deg)		80.47(1)		
β (deg)	98.50(2)	79.72(1)	106.15(1)	
γ (deg)		75.84(1)		
V (Å^3)	3127.6(15)	1739.9(3)	2782.1(8)	3475.0(8)
Z	4	2	4	4
dcal (g cm^{-3})	2.051	1.952	2.145	1.886
F(000)	1852	984	1712	1912
radiatn (Å)	0.71073	0.71073	0.71073	0.71073
T (K)	295	294	295	295
(μMo Kα), cm^{-1}	19.68	17.7	22.02	18.34
diffractometer	Siemens R3m/V	Siemens R3m/V	Siemens R3m/V	Siemens R3m/V
crystal size (mm)	0.40{10–1} × 0.22{010} × 0.30{0–11} × 0.30{0–1–1}	0.32{100} × 0.18{010} × 0.47{001} × 0.29{011} × 0.23{011}	0.14(010,010) × 0.42(001,00–1) × 0.42(101,–101) × 0.28(10–1,–101)	0.34 × 0.56 × 0.36
scan type	ω	ω	ω	ω
2θ range (deg)	4.0–50.0	4.0–55.0	4.0–55.0	4.0–60.0
scan width (deg)	1.20	1.40	1.50	1.30
scan speed (deg min^{-1})	2.93–29.30 in ω	2.93–29.30 in ω	2.93–29.30 in ω	2.93–29.30 in ω
abspn correctns	face-indexed numerical	face-indexed numerical	face-indexed numerical	ψ-scan semiempirical
transmission factors	0.6207–0.6960	0.5088–0.7650	0.5655–0.7397	0.4130–0.4724
reflns measured	5543	8055	3232	5295
reflns obsd ($F \geq 6\sigma(F)$)	4670	6565	3112	3979
R	0.0235	0.0291	0.0203	0.0299
Rw	0.0337	0.0459	0.0255	0.0334
weighting scheme, w^{-1}	$\sigma^2(F) + 0.0002F^2$	$\sigma^2(F) + 0.00155F^2$	$\sigma^2(F) + 0.00024F^2$	$\sigma^2(F) + 0.00001F^2$
max residuals, e Å^{-3}	0.41	0.46	0.46	0.81

Results and Discussion

Reaction of transition metal clusters with alkynes and 1,3-diynes proceeds most efficiently when lightly stabilized[28] or activated clusters[29] are employed. Under more forcing conditions the reaction frequently becomes nonselective affording a wide variety of stable products usually in low yield, including those arising from C–H activation,[30] H migration,[31] C–C coupling,[32] C–C bond cleavage,[33] and isomerization.[34] We have discovered that reaction of $Ru_4(CO)_{13}(\mu_3\text{-}PPh)$ (1) with a wide variety of alkynes and diynes proceeds under mild conditions, in the majority of cases yielding a single major product. In the case of unsymmetrical alkynes these reactions occur with high regiospecificity. Such facile addition of unsaturated hydrocarbyl ligands into a stable tetranuclear cluster represents a potentially powerful system for investigating framework reaction chemistry of this class of molecules. We note also that relatively few studies of the activation of small molecules at a square M_3X face have been carried out. Moreover, a square Ru_4 fragment provides a model for chemical transformations at the (100) face of metallic ruthenium.[35] Although ruthenium is a very important catalytic metal, models for the interaction of hydrocarbons with this (100) array are rare.[35,36]

The major product isolated from the reaction of 2,4-hexadiyne and 1 at 60 °C is $Ru_4(CO)_{10}(\mu\text{-}CO)_2\{\mu_4\text{-}\eta^1,\eta^1,\eta^2\text{-}P(Ph)(MeC{\equiv}C)C{\equiv}CMe\}$ (2c). In a similar reaction with 1,4-diphenylbutadiyne and 1,4-bis(trimethylsilyl)butadiyne

(28) (a) Foulds, G. A.; Johnson, B. F. G.; Lewis, J. *J. Organomet. Chem.* **1985**, *296*, 147. (b) Deeming A. J.; Kabir, S. S.; Nuel, D.; Powell, N. I. *Organometallics* **1989**, *8*, 717. (c) Arce, A. J.; Manzur, J.; Marquez, M.; DeSanctis, Y.; Deeming, A. J. *J. Organomet. Chem.* **1991**, *412*, 177. (d) Arce, A. J.; DeSanctis, Y.; Deeming, A. J.; Hardcastle, K. I.; Lee, R. *J. Organomet. Chem.* **1991**, *406*, 209. (e) Chen, H.; Johnson, B. F. G.; Lewis, J.; Raithby, P. R. *J. Organomet. Chem.* **1991**, *406*, 219. (f) Johnson, B. F. G.; Khattar, R.; Lahez, F. J.; Lewis, J.; Raithby, P. R. *J. Organomet. Chem.* **1987**, *319*, C51. (g) Braga, D.; Grepioni, F.; Johnson, B. F. G.; Lewis, J.; Lunniss, J. *J. Chem. Soc., Dalton Trans.* **1992**, 1101. (h) Aime, S.; Gobetto, R.; Milone, L.; Osella, D.; Violano, L.; Arce, A. J.; DeSanctis, Y. *Organometallics* **1991**, *10*, 2854.

(29) Rivomanana, S.; Lavigne, G.; Lugan, N.; Bonnet, J. J.; Yanez, R.; Mathieu, R. *J. Am. Chem. Soc.* **1989**, *111*, 8959.

(30) (a) Johnson, B. F. G.; Lewis, J.; Lunniss, J.; Braga, D.; Grepioni, *J. Organomet. Chem.* **1991**, *412*, 195. (b) Aime, S.; Milone, L.; Osella, D.; Valle, M. *J. Chem. Res., Synop.* **1978**, 77; *J. Chem. Res., Miniprint* **1978**, 785–797. (c) Gervasio, G.; Osella, D.; Valle M. *Inorg. Chem.* **1976**, *15*, 1221. (d) Boyar, E.; Deeming, A. J.; Felix, M. S. B.; Kabir, S. E.; Adatia, T.; Bhusate, R.; McPartlin, M.; Powell, H. R. *J. Chem. Soc., Dalton Trans.* **1989**, 5. (e) Deeming, A. J.; Hasso, S.; Underhill, M. *J. Organomet. Chem.* **1974**, *80*, C53.

(31) (a) Aime, S.; Milone, L.; Sappa, E.; Tiripicchio, A. *J. Chem. Soc., Dalton Trans.* **1977**, 227. (b) Raverdino, V.; Aime, S.; Milone, L.; Sappa, E. *Inorg. Chim. Acta* **1978**, *30*, 9.

(32) (a) Adams, R. D.; Babin, J. E.; Tasi, M.; Wang, J. G. *Organometallics* **1988**, *7*, 755. (b) Johnson, B. F. G.; Khattar, R.; Lewis, J.; Raithby, P. R. *J. Organomet. Chem.* **1987**, *335*, C17. (c) Adams, R. D.; Arafa, I.; Chen, G.; Lii, J. C.; Wang, J. G. *Organometallics* **1990**, *9*, 2350. (d) Fehlhammer, W. B.; Stolzenberg, H. In *Comprehensive Organometallics Chemistry*; Wilkinson, G., Stone, F. G. A., Abel, E., Eds.; Pergamon: Oxford, UK, 1982; Chapter 31.4. (e) Riaz, U.; Curtis, M. D.; Rheingold, A. L.; Haggerty, B. S. *Organometallics* **1990**, *9*, 2647.

(33) (a) Johnson, B. F. G.; Lewis, J.; Lunniss, J.; Braga, D.; Grepioni, F. *J. Chem. Soc., Chem. Commun.* **1988**, 972. (b) Braga, D.; Grepioni, F.; Johnson, B. F. G.; Lewis, J.; Lunniss, J. *J. Chem. Soc., Dalton Trans.* **1991**, 2223. (c) Park, J. T.; Shapley, J. R.; Churchill, M. R.; Bueno, C. *J. Am. Chem. Soc.* **1983**, *105*, 6182.

(34) (a) Evans, M.; Hursthouse, M.; Randall, E. W.; Rosenberg, E.; Milone, L.; Valle, M. *J. Chem. Soc., Chem. Commun.* **1972**, 545. (b) Fogg, D. E.; MacLaughlin, S. A.; Kwek, K.; Cherkas, A. A.; Taylor, N. J.; Carty, A. J. *J. Organomet. Chem.* **1988**, *352*, C17.

(35) (a) Knox, S. A. R.; Lloyd, B. R.; Orpen, A. G.; Vinas, J. M.; Weber, M. *J. Chem. Soc., Chem. Commun.* **1987**, 1498. (b) Knox, S. A. R.; Lloyd, B. R.; Morton, D. A. V.; Nicholls, S. M.; Orpen, A. G.; Vinas, J. M.; Weber, M.; Williams, G. K. *J. Organomet. Chem.* **1990**, *394*, 385.

(36) Johnson, B. F. G.; Lewis, J.; Gallup, M.; Martinelli, M. *Faraday Discuss.* **1991**, *92*, 241.

Scheme I

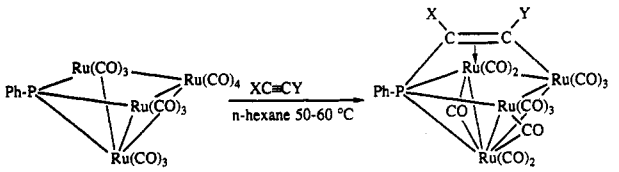

1

X = C≡CR, Y = R
X = R, Y = C≡C R
R =Ph, 2a; R = $SiMe_3$, 2b
R = Me, 2c

the corresponding products **2a** and **2b** were isolated in high yield. The reaction of **1** with 1,4-diphenylbutadiyne proceeded more efficiently at lower temperature over a longer time, these conditions acting to reduce a side product of alkyne trimerization $Ru_4(CO)_8(\mu_4\text{-PPh})[\eta^1,\eta^1,\eta^2,\eta^2\text{-(Ph)CC(C≡CPh)C(Ph)C-}\eta^4\text{-CC(Ph)C(Ph)C(C≡CPh)}]$ (**8**) recently isolated and characterized.[25]

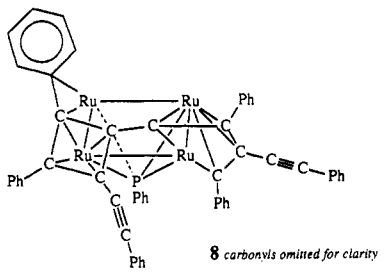

8 *carbonyls omitted for clarity*

Compounds **2a–c** have been characterized spectroscopically (^{31}P, ^1H, and ^{13}C), and in each case a high field shift of the phosphinidene resonance indicated an extensive modification of its bonding characteristics. The $^{31}P\{^1H\}$ resonance of **1** appears at δ = 409 and those of **2a–c** at approximately δ = 45 ($\Delta\delta \approx -360$ ppm). Similar large shifts have been correlated with the presence of a more open skeletal structure.[37] We have recently reported a similar high field shift (δ = 60 ppm) for a five-coordinate phosphido bridge derived from the electron-rich cluster $Ru_4(CO)_{13}(\mu\text{-PPh}_2)_2$.[38] Solution infrared spectra of **2a–c** displayed very low frequency carbonyl absorption bands characteristic of CO ligands bridging M–M bonds, while the region containing the absorptions due to the terminal carbonyl ligands possessed similar symmetry to that of *nido*-$Ru_4(CO)_{12}\{\mu_4\text{-}\eta^1,\eta^1,\eta^2\text{-P(Ph)CPhCPh}\}$ (**6**).[15] The observed spectroscopic data indicated that **2a–c** were structurally similar to the previously characterized cluster **6**, however, asymmetry-induced by the coordination of a single diyne triple bond leads to the possibility of regioisomeric clusters (either X = R, Y = C≡CR or X = C≡CR, Y = R, where R = Ph, Me, $SiMe_3$) (Scheme I). We found only a single isomeric product under the thermal conditions employed but to unequivocally establish the regiochemistry of addn. to **1** we carried out a single-crystal X-ray analysis of **2c**.

A perspective view of the molecular structure of **2c** together with the atomic numbering scheme is illustrated in Figure 1. Table II contains final positional parameters while selected interatomic distances and angles are given in Table III. The overall structure is similar to that of **6**

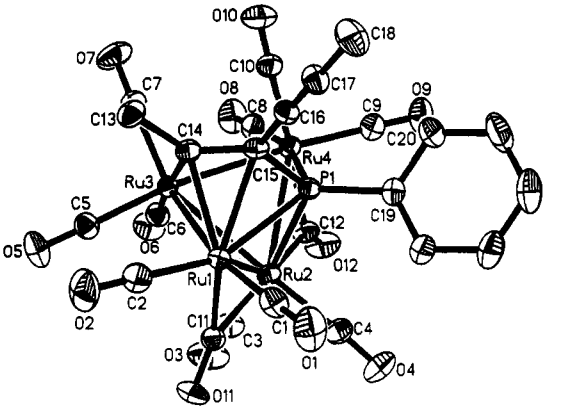

Figure 1. Perspective view of the molecular structure of *nido*-$Ru_4(CO)_{10}(\mu\text{-CO})_2\{\mu_4\text{-}\eta^1,\eta^1,\eta^2\text{-P(Ph)C(C≡CMe)CMe}\}$ (**2c**).

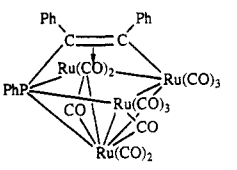

6

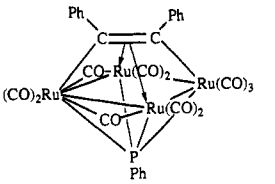

7

with the stereochemistry about the $\mu_3\text{-}\eta^2$ bonded acetylene being geminal with respect to the pendant triple bond and the phosphinidene.

The basic square pyramidal framework of the precursor **1** is retained with five metal–metal bonds [Ru(1)–Ru(2) = 2.764(1) Å, Ru(1)–Ru(3) = 2.865(1) Å, Ru(2)–Ru(3) = 2.860(1) Å, Ru(2)–Ru(4) = 2.881(1) Å, Ru(3)–Ru(4) = 2.910(1) Å] and three metal–phosphorus bonds. The latter [Ru(1)–P(1) = 2.533(1) Å, Ru(2)–P(1) = 2.486(1) Å, Ru(4)–P(1) = 2.351(1) Å] are marginally elongated compared to those of **1** (Ru–P average 2.335 Å) though well within bonding distance and similar to those of a previously reported five-coordinate phosphido bridge.[38] Ten of the 12 carbonyl ligands in **2c** are terminally bound to the ruthenium atoms, while the remaining two [C(11)O(11) and C(12)O(12)] bridge Ru(1)–Ru(2) and Ru(2)–Ru(4), respectively [Ru(1)–C(11) = 1.965(4) Å, Ru(2)–C(11) = 2.238(4) Å, Ru(2)–C(12) = 2.070(5) Å, Ru(4)–C(12) = 2.141(4) Å], reflecting the electronic inbalance that would otherwise be associated with Ru(1), Ru(2), and Ru(4) in their absence. The principal structural feature of interest in **2c** is the coordinated 1,3-diyne (C(13)–C(18)) attached to the open Ru_2P triangle of the Ru_3P square face of **1**. Although one of the skeletal atoms involved in the bonding is a main group atom, the mode of attachment is representative of $\mu_3\text{–}\eta^2$-coordination to an open M_3 triangle.[39] Thus, the phosphinidene behaves, in this case, similar to a typical metal atom. Atoms Ru(3) and P(1) are σ-bound to the acetylenic carbon atoms C(14) and C(15) [Ru(3)–C(14) = 2.147(4) Å, P(1)–C(15) = 1.805(4) Å], while Ru(1) is involved in an η^2-interaction to the same fragment [Ru(1)–C(14) = 2.247(4) Å and Ru(1)–C(15) = 2.304(4) Å]. The C(14)–C(15) bond length of 1.376(5) Å is consistent with the reduction in bond order expected upon coordination of the acetylenic triple bond. The C–C bond length of the pendant acetylenic fragment [C(16)–C(17) = 1.172(6) Å] is within the range observed for other

(37) Carty, A. J.; MacLaughlin, S. A.; Nucciarone, D. In *Phosphorus-31 NMR Spectroscopy in Stereochemical Analysis: Organic Compounds and Metal Complexes*; Verkade, J. G., Quinn, L. D., Eds.; VCH: New York, 1987; Chapter 16, pp 559–619.

(38) Corrigan, J. F.; Doherty, S.; Taylor, N. J.; Carty, A. J. *J. Am. Chem. Soc.* **1992**, *114*, 7557.

(39) MacLaughlin, S. A.; Johnson, J. P.; Taylor, N. J.; Carty, A. J.; Sappa, E. *Organometallics* **1983**, *2*, 352.

Table II. Atomic Coordinates (×10⁴) and Equivalent Isotropic Displacement Coefficients (Å² × 10³) for $Ru_4(CO)_{10}(\mu\text{-}CO)_2\{\mu_4\text{-}\eta\text{-}\eta^1,\eta^2\text{-}P(Ph)C(C{\equiv}CMe)CMe\}$ (2c)

	x	y	z	U(eq)[a]
Ru(1)	3920.3(3)	1117.4(1)	−173.1(2)	31.0(1)
Ru(2)	4046.5(3)	2123.2(1)	672.7(3)	33.8(1)
Ru(3)	1451.2(3)	1736.5(1)	−363.6(2)	33.2(1)
Ru(4)	1791.5(3)	2018.9(1)	1877.1(3)	34.7(1)
P(1)	3364.9(10)	1342.6(4)	1656.4(8)	31.5(3)
O(1)	6462(4)	459(2)	497(3)	79(2)
O(2)	3563(4)	543(2)	−2280(3)	82(2)
O(3)	4339(5)	3094(2)	−662(4)	94(2)
O(4)	6968(3)	2241(2)	1785(3)	76(2)
O(5)	1451(4)	1546(2)	−2721(3)	71(1)
O(6)	1029(4)	2922(1)	−760(3)	70(1)
O(7)	−1613(3)	1546(2)	−359(3)	83(2)
O(8)	−347(4)	2913(2)	1437(3)	76(2)
O(9)	2578(4)	2158(2)	4280(3)	74(2)
O(10)	−410(4)	1181(2)	2034(3)	80(2)
O(11)	5567(3)	1892(1)	−1264(3)	57(1)
O(12)	3443(4)	3055(1)	2016(3)	75(2)
C(1)	5526(5)	702(2)	234(3)	47(2)
C(2)	3697(5)	755(2)	−1496(4)	49(2)
C(3)	4215(5)	2724(2)	−176(4)	55(2)
C(4)	5868(5)	2200(2)	1378(4)	48(2)
C(5)	1471(5)	1608(2)	−1838(4)	47(2)
C(6)	1251(4)	2488(2)	−597(3)	46(2)
C(7)	−471(5)	1627(2)	−366(4)	51(2)
C(8)	428(5)	2594(2)	1605(3)	49(2)
C(9)	2277(5)	2116(2)	3391(4)	49(2)
C(10)	396(5)	1490(2)	1950(3)	50(2)
C(11)	4901(4)	1726(2)	−659(3)	39(1)
C(12)	3249(4)	2630(2)	1704(4)	46(2)
C(13)	892(4)	497(2)	−637(3)	46(2)
C(14)	1740(4)	916(2)	23(3)	36(1)
C(15)	2526(4)	780(2)	972(3)	35(1)
C(16)	2652(4)	256(2)	1446(3)	37(1)
C(17)	2744(5)	−152(2)	1884(3)	44(1)
C(18)	2860(6)	−676(2)	2398(4)	66(2)
C(19)	4520(4)	1083(2)	2780(3)	38(1)
C(20)	3970(5)	925(2)	3671(4)	54(2)
C(21)	4829(7)	719(3)	4527(4)	83(3)
C(22)	6206(7)	656(3)	4498(5)	85(3)
C(23)	6754(6)	810(2)	3621(5)	71(2)
C(24)	5918(5)	1031(2)	2765(4)	50(2)
solvent				
C(1S)	416(9)	136(4)	4064(7)	115(4)
C(2S)	−159(8)	−340(4)	4180(7)	112(4)
C(3S)	−565(8)	−473(3)	5132(10)	120(4)

[a] Equivalent isotropic U defined as one-third of the trace of the orthogonalized U_{ij} tensor.

structurally characterized 1,3-diyne containing clusters.[40] A similar regiospecific C–S bond forming reaction on the cluster $Os_4(CO)_{12}(\mu_3\text{-}S)$ recently reported by Adams was shown to exhibit structural similarities to those of **2a–c**, although the selectivity of formation of this tetraosmium cluster was lowered by the presence of a competing reaction involving a 1,2-hydrogen migration affording a well-known vinylidene type cluster.[14a]

Four acetylenic resonances were assigned in the J-modulated $^{13}C\{^1H\}$ NMR spectra of **2a–c**. For instance, the $^{13}C\{^1H\}$ NMR spectrum of **2a** contained three signals characteristic of quaternary carbons in the region δ 88–92 ppm, the remaining acetylenic resonance appearing at low field (δ = 185.3). All four acetylenic resonances couple to phosphorus [δ = 185.2, J_{PC} = 30.0 Hz; δ = 92.0, J_{PC} = 5.0 Hz; δ = 91.5, J_{PC} = 11.0 Hz; δ = 89.0, J_{PC} = 40.0 Hz]. That one of the acetylenic carbon resonances appears at such low field (and in most instances in the region associated

(40) (a) Bruce, M. I.; Koutsantonis, G. A.; Tiekink, E. R. T. *J. Organomet. Chem.* **1991**, *407*, 391. (b) Adams, C. J.; Bruce, M. I.; Hurn, E.; Tiekink, E. R. T. *J. Chem. Soc., Dalton Trans.* **1992**, 1157. (c) Worth, G. H.; Robinson, B. H.; Simpson, J. *Organometallics* **1992**, *11*, 501.

Table III. Selected Interatomic Bond Distances (Å) and Angles (deg) for $Ru_4(CO)_{10}(\mu\text{-}CO)_2\{\mu_4\text{-}\eta^1,\eta^1,\eta^2\text{-}P(Ph)C(C{\equiv}CMe)CMe\}$ (2c)

Ru(1)–Ru(2)	2.764(1)	Ru(1)–Ru(3)	2.865(1)
Ru(2)–Ru(4)	2.881(1)	Ru(3)–Ru(4)	2.910(1)
Ru(2)–Ru(3)	2.860(1)	Ru(1)–P(1)	2.533(1)
Ru(2)–P(1)	2.486(1)	Ru(4)–P(1)	2.351(1)
Ru(1)–C(14)	2.247(5)	Ru(1)–C(15)	2.304(4)
Ru(3)–C(14)	2.147(5)	P(1)–C(15)	1.805(4)
C(13)–C(14)	1.523(5)	C(14)–C(15)	1.376(5)
C(15)–C(16)	1.458(5)	C(16)–C(17)	1.172(7)
C(17)–C(18)	1.478(7)		
Ru(2)–Ru(1)–Ru(3)	61.0(1)	Ru(1)–Ru(2)–Ru(3)	61.2(1)
Ru(1)–Ru(3)–Ru(2)	57.8(1)	Ru(2)–Ru(3)–Ru(4)	59.9(1)
Ru(3)–Ru(2)–Ru(4)	60.9(1)	Ru(1)–Ru(2)–Ru(4)	97.4(1)
Ru(1)–Ru(3)–Ru(4)	94.5(1)	Ru(2)–Ru(4)–Ru(3)	59.2(1)
Ru(3)–Ru(1)–P(1)	70.2(1)	Ru(2)–Ru(1)–P(1)	55.8(1)
Ru(1)–Ru(2)–P(1)	57.4(1)	Ru(4)–Ru(2)–P(1)	51.3(1)
Ru(2)–Ru(4)–P(1)	55.6(1)	Ru(3)–Ru(4)–P(1)	71.7(1)
Ru(3)–Ru(2)–P(1)	70.9(1)	Ru(1)–P(1)–Ru(2)	66.8(1)
Ru(1)–P(1)–Ru(4)	120.5(1)	Ru(2)–P(1)–Ru(4)	73.1(1)
Ru(1)–P(1)–C(15)	61.5(1)	Ru(4)–P(1)–C(15)	112.0(1)
Ru(2)–P(1)–C(19)	120.3(1)		

with carbonyl resonances) was established by examination of the $^{13}C\{^1H\}$ NMR spectrum of the parent cluster $Ru_4(CO)_{10}(\mu\text{-}CO)_2\{\mu_4\text{-}\eta^1,\eta^1,\eta^2\text{-}P(Ph)C(H)CH\}$ (**9**).[25] The μ_3-

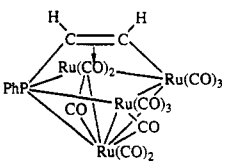

9

η^2-acetylenic carbon resonances were readily identified (δ = 165.6, J_{PC} = 20.0 Hz, δ = 89.8, J_{PC} = 38.0 Hz) assuring correct assignment of the corresponding resonances in **2a–c**. The acetylenic carbon bound to phosphorus is expected to have associated with it a degree of sp^2 character and therefore show a $^1J_{PC}$ similar to that of an ipso carbon of a P–Ph fragment. For $Ru_4(CO)_{10}(\mu\text{-}CO)_2\{\mu_4\text{-}\eta^1,\eta^1,\eta^2\text{-}P(Ph)C(H)CH\}$ (**9**) the resonance at δ 89.8 compares favorably with δ values for the alkyne carbon atoms bound to phosphorus in clusters **2a–c**.

Skeletal Transformations of 2a and 2c. When heated at reflux (67 °C) in hexane clusters **2a** and **2c** readily undergo skeletal transformations concomitant with CO loss to afford $Ru_4(CO)_{10}(\mu\text{-}CO)(\mu_4\text{-}PPh)\{\mu_4\text{-}\eta^1,\eta^1,\eta^2,\eta^2\text{-}(RC{\equiv}C)C{\equiv}C(R)\}$ (R = Ph, **3a**, R = Me, **3c**). A compound with spectroscopic properties similar to those of **3a** and **3c** has been identified in the reaction mixture of 1,4-bis(trimethylsilyl)butadiyne with **1** although **3b** could not be obtained from the direct thermolysis of hydrocarbon solutions of **2b** (**4b** was the only major product from these reactions, vide infra). For **3a–c** a low-frequency infrared absorption band (ν(CO): μ_2-CO 1858 cm^{-1}) characteristic of a bridging carbonyl was present, and the symmetry of the higher frequency terminal carbonyl absorptions inferred a structure similar to $Ru_4(CO)_9(\mu\text{-}CO)_2(\mu_4\text{-}PPh)\{\mu_4\text{-}\eta^1,\eta^1,\eta^2,\eta^2\text{-}PhC{\equiv}CPh\}$ (**7**).[15] Unfortunately, vastly disparate values of the phosphorus chemical shifts in these compounds could not reinforce these structural predictions (δ = 352 for **7**, δ = 242–250 for **3a–c**). A structure similar to that of **7** would require an electron count of 62 CVE, two short of that required by the EAN rule. We and others

have prepared similar "electron-deficient"[14d,18d,41] square planar clusters, and these have been the subject of intense theoretical interest.[42] The $^{31}P\{^1H\}$ signals of these clusters lie markedly upefield of those of **1** (δ = 409 ppm)[6] and normal 64 electron clusters containing μ_4-PPh-stabilizing groups.[43] These features may indicate the presence of unusual electronic effects since ^{31}P shifts of these ligands capping Ru_4 square faces usually appear at much lower fields.[44] Vahrenkamp and Haines have noted similar high-field shifts for the ^{31}P NMR resonances of the related unsaturated 62-electron clusters $M_4(CO)_{10}(\mu\text{-}CO)(\mu_4\text{-}PPh)_2$ (M = Fe, Ru).[44,45] Vahrenkamp attributed these unusual shifts to anisotropy, the effective magnetic field above the center of the M_4 plane, being similar to the anisotropy observed in aromatic rings. Such effects may be the cause of the unusual chemical shifts encountered in the ^1H NMR spectra of compounds **3a–c**. We observed high-field shifts of the aromatic protons, these shifts being far in excess of those normally displayed by μ_4-PPh ligands.[46] For instance, in the ^1H NMR spectrum of **2c** two sets of phenyl resonances were observed δ = 7.35 (3H) assigned as the meta and para hydrogen atoms and δ = 7.15 (2H) for the ortho hydrogen atoms. Compound **3c** showed two resonances with similar multiplicity to those of **2c** the one assigned to the meta and para hydrogen atoms (δ = 7.12, $\Delta\delta$ = 0.23 ppm) being shifted much less than that associated with the ortho hydrogen atoms (δ = 6.44, $\Delta\delta$ = 0.71 ppm). Cluster **3a** exhibited similar characteristics in its ^1H NMR spectra. The $^{13}C\{^1H\}$ NMR spectra of **3a** and **3c** (δ C ipso = 137.0 ppm and δ C ipso = 133.3 ppm for **3a** and **3c**, respectively) are also unusual. Similar effects might be expected on the hydrocarbon ligand μ_4-bonded to the opposite face of the Ru_4 plane, but the lack of $^{13}C\{^1H\}$ NMR data for acetylenic ligands μ_4–η^2 bound to M_4 square faces precludes any further comparisons.

The downfield shifts of the ^{31}P resonances associated with the transformations **2a–c** to **3a–c** ($\Delta\delta$ = 200 ppm) are indicative of a severe structural rearrangement at phosphorus, and these $\delta(^{31}P)$ values are in the region commonly encountered for 62 CVE species of the type $Ru_4(CO)_{10}(\mu\text{-}CO)(\mu_4\text{-}X)(\mu_4\text{-}Y)$.[41] Compounds **3a** and **3c** were characterized by single-crystal X-ray studies to unequivocally establish the nature of the cluster bound phosphinidene and the regiospecificity of rearrangement. A perspective view of the molecular structure of **3a** together with the atomic numbering scheme is illustrated in Figure 2. The structure of **3c** is given in Figure 3. Tables IV and VI contain the atomic coordinates for **3a** and **3c** respectively, while bond distances and angles for **3a** and **3c** are listed in Tables V and VII, respectively. Qualitatively, both

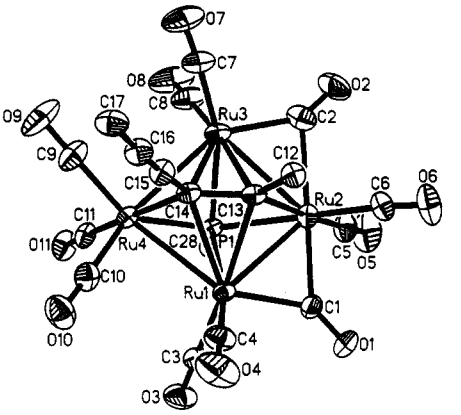

Figure 2. Perspective view of the molecular structure of *closo*-$Ru_4(CO)_{10}(\mu\text{-}CO)(\mu_4\text{-}PPh)\{\mu_4\text{-}\eta^1,\eta^1,\eta^2,\eta^2\text{-}(PhC{\equiv}C)\text{-}C{\equiv}CPh\}$ (**3a**). A projection illustrating the pentagonal bipyramidal nature of the M_4PC_2 skeletal framework (phenyl rings omitted for clarity).

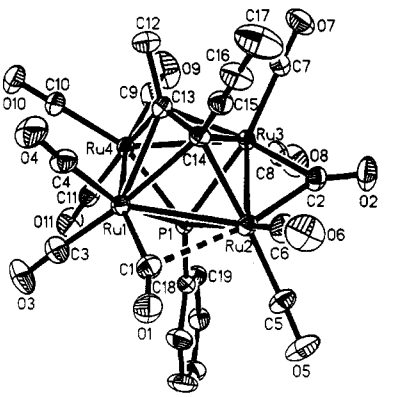

Figure 3. Perspective view of the molecular structure of *closo*-$Ru_4(CO)_{10}(\mu\text{-}CO)(\mu_4\text{-}PPh)\{\mu_4\text{-}\eta^1,\eta^1,\eta^2,\eta^2\text{-}(MeC{\equiv}C)\text{-}C{\equiv}CMe\}$ (**3c**). A projection emphasizing the μ_4–η^2-coordination geometry of the 1,3-diyne ligand (phenyl ring omitted for clarity).

clusters consist of distorted square planar arrangements of metal atoms capped on one side by a μ_4-PPh group and on the other by a μ_4-η^2-RC≡CR′ (R = Ph, R′ = C≡CPh **3a**; R = C≡CMe, R′ = Me **3c**) acetylene. A comparison of Figures 2 and 3 reveals that these clusters have undergone opposite regiochemistry of rearrangement with respect to Ru(2). For instance, the pendant acetylenic unit C(15)–C(16) in cluster **3a** possesses a vicinal disposition with respect to Ru(2) about C(13)–C(14) whereas the transformation undertaken by **2c** renders C(15)–C(16) geminal with respect to Ru(2) about C(13)–C(14). As a consequence there are many other structural differences, and these are described below. Two of the M–M bonds in **3a** are similar and of normal length for Ru–Ru single bonds in tetranuclear clusters [Ru(1)–Ru(4) = 2.851(1) Å, Ru(3)–Ru(4) = 2.873(1) Å] while the remaining two, those associated with the bridging carbonyl ligands, are significantly shorter [Ru(1)–Ru(2) = 2.742(1) Å, Ru(2)–Ru(3) = 2.786(1) Å]. This pattern of two normal and two shortened metal–metal bonds is similar to that found in **7**[15] [normal, 2.8746(5) Å, 2.8515(5) Å; shortened, 2.7777(5) Å, 2.7432(5) Å] although a different distribution of three normal and one shortened M–M bond was found in the closely related electron-deficient square-planar cluster $Os_4(CO)_{11}(\mu_4\text{-}S)(\mu_4\text{-}\eta^2\text{-}HC_2CO_2Me)$.[14b] This latter distribution of bond types, one localized short multiple M–M bond and three normal bonds, is similar to the

(41) (a) van Gastel, F.; Agocs, L.; Cherkas, A. A.; Corrigan, J. F.; Doherty, S.; Ramachandran, R.; Taylor, N. J.; Carty, A. J. *J. Cluster Sci.* **1991**, *2*, 131. (b) Braunstein, P. *New J. Chem.* **1986**, *10*, 365. (c) Adams, R. D.; Wolfe, T. A.; Wu, W. *Polyhedron* **1991**, *10*, 447. (d) Mathur, P.; Thimmappa, B. H. S.; Rheingold, A. L. *Inorg. Chem.* **1990**, *29*, 4658. (e) Adams, R. D.; Babin, J. E.; Tasi, M. *Inorg. Chem.* **1986**, *25*, 4514. (f) Adams, R. D.; Babin, J. E.; Estrada, J.; Wang, J. G.; Hall, M. B.; Low, A. A. *Polyhedron* **1989**, *8*, 1885. (g) Mathur, P.; Charkrabarty, D.; Hossain, M. M. *J. Organomet. Chem.* **1991**, *418*, 415. (h) Mathur, P.; Mavunkal, I. J.; Rugmini, V.; Mahon, M. F. *Inorg. Chem.* **1990**, *29*, 4838.

(42) (a) Halet, J. F.; Hoffmann, R.; Saillard, J. Y. *Inorg. Chem.* **1985**, *25*, 1695. (b) Jaeger, J. T.; Field, J. S.; Collison, D.; Speck, G. P.; Peake, B. M.; Hahnle, J.; Vahrenkamp, H. *Organometallics* **1988**, *7*, 1753.

(43) Corrigan, J. F.; Doherty, S.; Taylor, N. J.; Carty, A. J. *J. Chem. Soc., Chem. Commun.* **1991**, 1640.

(44) Jaeger, T.; Aime, S.; Vahrenkamp, H. *Organometallics* **1986**, *5*, 245.

(45) Field, J. S.; Haines, R. J.; Smit, D. N. *J. Chem. Soc., Dalton Trans.* **1988**, 1315.

(46) Deeming, A. J.; Doherty, S.; Powell, N. I. *Inorg. Chim. Acta* **1992**, *198–200*, 469.

Table IV. Atomic Coordinates (×10⁴) and Equivalent Isotropic Displacement Coefficients (Å² × 10³) for $Ru_4(CO)_{10}(\mu\text{-}CO)(\mu_4\text{-}PPh)\{\mu_4\text{-}\eta^1,\eta^1,\eta^2,\eta^2\text{-}(PhC{\equiv}C)C{\equiv}CPh\}$ (3a)

	x	y	z	U(eq)[a]
Ru(1)	969.8(3)	2673.2(3)	1626.8(1)	36.5(1)
Ru(2)	-1833.1(3)	3766.9(3)	2276.4(1)	42.3(1)
Ru(3)	-1956.1(3)	910.9(3)	2720.0(1)	42.1(1)
Ru(4)	577.3(3)	-199.7(3)	1774.6(1)	37.9(1)
P(1)	-1313.6(9)	1893.7(9)	1572.7(4)	36.2(3)
O(1)	-7(5)	5906(3)	1456(2)	86(2)
O(2)	-4628(4)	3050(5)	3338(2)	90(2)
O(3)	1957(4)	2991(4)	146(2)	82(2)
O(4)	4041(4)	2997(6)	1815(2)	101(2)
O(5)	-4422(5)	5739(5)	1627(2)	107(2)
O(6)	-2126(5)	6041(5)	3185(2)	97(2)
O(7)	-1762(6)	-1112(5)	4015(2)	105(2)
O(8)	-4122(6)	-686(6)	2430(2)	118(3)
O(9)	996(6)	-3092(4)	2651(2)	114(2)
O(10)	3947(4)	-654(4)	1311(2)	83(2)
O(11)	-90(4)	-1281(3)	554(2)	69(1)
C(1)	-119(5)	4751(4)	1660(2)	52(1)
C(2)	-3501(5)	2614(6)	3022(2)	65(2)
C(3)	1594(4)	2857(4)	704(2)	49(1)
C(4)	2886(5)	2866(5)	1756(2)	58(2)
C(5)	-3438(5)	5009(5)	1853(2)	65(2)
C(6)	-2040(5)	5163(5)	2876(2)	58(2)
C(7)	-1853(5)	-330(5)	3546(2)	64(2)
C(8)	-3331(6)	-75(6)	2541(2)	74(2)
C(9)	821(6)	-2036(5)	2309(2)	68(2)
C(10)	2676(5)	-457(5)	1463(2)	57(2)
C(11)	169(5)	-918(4)	1001(2)	50(1)
C(12)	188(4)	2663(4)	3380(2)	43(1)
C(13)	-117(3)	2193(4)	2766(2)	37(1)
C(14)	674(4)	817(4)	2610(2)	38(1)
C(15)	1700(4)	-9(4)	3054(2)	45(1)
C(16)	2512(4)	-696(4)	3435(2)	50(1)
C(17)	3435(4)	-1474(5)	3926(2)	54(1)
C(18)	-649(6)	2377(6)	3998(2)	71(2)
C(19)	-319(7)	2762(7)	4569(2)	83(3)
C(20)	803(5)	3472(5)	4533(2)	65(2)
C(21)	1617(5)	3795(6)	3922(2)	68(2)
C(22)	1309(5)	3388(5)	3352(2)	56(2)
C(23)	4266(6)	-2841(7)	3860(3)	86(2)
C(24)	5156(7)	-3571(9)	4344(4)	122(3)
C(25)	5190(8)	-2914(11)	4889(3)	121(4)
C(26)	4385(8)	-1567(9)	4943(3)	107(4)
C(27)	3483(7)	-825(7)	4472(3)	81(2)
C(28)	-2357(4)	2227(4)	876(2)	39(1)
C(29)	-2334(4)	3477(4)	425(2)	50(1)
C(30)	-3173(5)	3761(5)	-99(2)	63(2)
C(31)	-3990(5)	2809(5)	-182(2)	66(2)
C(32)	-3992(5)	1588(6)	255(2)	63(2)
C(33)	-3178(4)	1283(5)	786(2)	54(1)

[a] Equivalent isotropic U defined as one-third of the trace of the orthogonalized U_{ij} tensor.

pattern in the closely related electron-deficient clusters $Ru_4(CO)_{10}(\mu\text{-}CO)(\mu_4\text{-}X)(\mu_4\text{-}Y)$(X = PPh, Y = S, Se, Te).[41a] Close examination of the metal atom skeleton of **3b** reveals a different distribution of M–M bonds, with only a single shortened M–M bond [Ru(2)–Ru(3) = 2.741(1) Å] symmetrically bridged by a carbonyl group [Ru(2)–C(12) = 2.050(5) Å, Ru(3)–C(12) = 2.274(5) Å]. The three remaining Ru–Ru bond lengths are longer [Ru(1)–Ru(2) = 2.807(1) Å, Ru(1)–Ru(4) = 2.807 (1) Å, Ru(3)–Ru(4) = 2.893(1) Å] but within the range expected for M–M bonds in Ru_4 clusters. This pattern of bond lengths more nearly parallels those found in the series $Ru_4(CO)_{10}(\mu\text{-}CO)(\mu_4\text{-}X)(\mu_4\text{-}Y)$[41] described earlier. The difference in M–M bonding between clusters **3a** and **3c** is reflected in the distribution of their bridging carbonyl ligands. Those of **3a** display less asymmetry [Δ(Ru–C) for C(11)–O(11) = 0.133(1) Å; C(12)–O(12) = 0.321(1) Å] while the equivalent parameter associated with **3c** is much larger [Δ(Ru–C) for

Table V. Selected Interatomic Bond Distances (Å) and Angles (deg) for $Ru_4(CO)_{10}(\mu\text{-}CO)(\mu_4\text{-}PPh)\{\mu_4\text{-}\eta^1,\eta^1,\eta^2,\eta^2\text{-}(PhC{\equiv}C)C{\equiv}CPh\}$ (3a)

Ru(1)–Ru(2)	2.742(1)	Ru(1)–Ru(4)	2.851(1)
Ru(2)–Ru(3)	2.786(1)	Ru(3)–Ru(4)	2.873(1)
Ru(1)–P(1)	2.437(1)	Ru(2)–P(1)	2.408(1)
Ru(3)–P(1)	2.419(1)	Ru(4)–P(1)	2.363(1)
Ru(1)–C(13)	1.871(4)	Ru(1)–C(14)	2.494(3)
Ru(2)–C(13)	2.176(3)	Ru(3)–C(13)	2.361(4)
Ru(4)–C(14)	2.139(4)	C(13)–C(14)	1.411(5)
C(12)–C(13)	1.501(5)	C(15)–C(16)	1.189(5)
C(14)–C(15)	1.438(5)	C(16)–C(17)	1.433(6)
Ru(2)–Ru(1)–Ru(4)	95.2(1)	Ru(1)–Ru(2)–Ru(3)	85.6(1)
Ru(2)–Ru(3)–Ru(4)	93.8(1)	Ru(1)–Ru(4)–Ru(3)	82.0(1)
Ru(1)–P(1)–Ru(3)	101.4(1)	Ru(1)–P(1)–Ru(2)	68.9(1)
Ru(2)–P(1)–Ru(4)	120.0(1)	Ru(1)–P(1)–Ru(4)	72.9(1)
Ru(2)–P(1)–Ru(3)	70.6(1)	Ru(3)–P(1)–Ru(4)	73.9(1)
C(12)–C(13)–C(14)	117.2(3)	C(13)–C(15)–C(15)	117.0(3)

Table VI. Atomic Coordinates (×10⁴) and Equivalent Isotropic Displacement Coefficients (Å² × 10³) for $Ru_4(CO)_{10}(\mu\text{-}CO)(\mu_4\text{-}PPh)\{\mu_4\text{-}\eta^1,\eta^1,\eta^2,\eta^2\text{-}(MeC{\equiv}C)C{\equiv}CMe\}$ (3c)

	x	y	z	U(eq)[a]
Ru(1)	3167.7(4)	2105.1(2)	1060.4(3)	32.1(1)
Ru(2)	1225.9(5)	3220.0(2)	399.8(3)	36.1(1)
Ru(3)	0	1653.8(2)	0	31.7(1)
Ru(4)	2078.3(4)	569.9(2)	210.0(3)	32.8(1)
P(1)	1827(1)	2030.0(8)	-350.2(8)	31.0(3)
O(1)	3955(5)	4036(3)	1335(5)	79(2)
O(2)	-1447(5)	3341(3)	-146(5)	75(2)
O(3)	5239(5)	1646(5)	418(4)	85(3)
O(4)	4405(6)	1619(5)	2918(3)	85(2)
O(5)	1205(7)	4672(4)	-897(4)	84(2)
O(6)	1148(7)	4707(4)	1666(4)	87(3)
O(7)	-1948(5)	858(4)	629(5)	79(2)
O(8)	-1456(5)	1227(5)	-1777(3)	83(2)
O(9)	177(7)	-804(5)	-425(7)	118(4)
O(10)	3614(6)	-668(4)	1563(4)	85(2)
O(11)	3396(6)	126(4)	-1111(3)	72(2)
C(1)	3457(6)	3376(4)	1183(5)	52(2)
C(2)	-540(5)	2970(3)	5(4)	43(2)
C(3)	4478(5)	1815(5)	676(4)	51(2)
C(4)	3979(6)	1800(4)	2230(4)	48(2)
C(5)	1205(6)	4130(4)	-403(4)	51(2)
C(6)	1164(6)	4151(4)	1209(4)	54(2)
C(7)	-1218(5)	1157(4)	404(4)	43(2)
C(8)	-915(5)	1396(4)	-1100(4)	51(2)
C(9)	866(6)	-270(5)	-176(6)	64(2)
C(10)	3039(5)	-222(4)	1064(4)	49(2)
C(11)	2898(5)	260(4)	-631(4)	47(2)
C(12)	1342(7)	586(4)	1925(4)	55(2)
C(13)	1506(4)	1175(3)	1221(3)	36(1)
C(14)	1333(4)	2099(3)	1308(3)	34(1)
C(15)	1056(5)	2415(4)	2064(3)	45(2)
C(16)	896(7)	2698(5)	2695(4)	58(2)
C(17)	700(12)	3084(8)	3473(7)	103(5)
C(18)	2080(4)	2282(3)	-1367(3)	37(1)
C(19)	1532(5)	1784(4)	-2087(3)	42(2)
C(20)	1701(7)	2002(5)	-2868(4)	55(2)
C(21)	2427(7)	2694(6)	-2937(5)	70(3)
C(22)	2967(8)	3197(6)	-2228(6)	75(3)
C(23)	2812(6)	2989(5)	-1436(4)	59(2)

[a] Equivalent isotropic U defined as one-third of the trace of the orthogonalized U_{ij} tensor.

C(11)–O(11) = 0.676 Å, C(12)–O(12) = 0.024 Å]. The latter value of 0.024 Å is a clear indication of the extent of localization of the multiple bond character at Ru(2)–Ru(3). A further structural feature of primary importance is the bonding of the 1,3 diyne ligand attached now to the Ru_4 square face through σ- and π-interactions, with the μ_4-PPh ligand supporting the apical position. In both clusters the single acetylenic triple bond is coordinated

Table VII. Selected Interatomic Bond Distances (Å) and Angles (deg) for $Ru_4(CO)_{10}(\mu\text{-}CO)(\mu_4\text{-}PPh)\{\mu_4\text{-}\eta^1,\eta^1,\eta^2,\eta^2\text{-}(MeC{\equiv}C)C{\equiv}CMe\}$ (3c)

Ru(1)–Ru(2)	2.807(1)	Ru(1)–Ru(4)	2.807(1)
Ru(2)–Ru(3)	2.741(1)	Ru(3)–Ru(4)	2.893(1)
Ru(1)–P(1)	2.407(1)	Ru(2)–P(1)	2.380(1)
Ru(3)–P(1)	2.447(1)	Ru(4)–P(1)	2.356(1)
Ru(1)–C(13)	2.487(5)	Ru(1)–C(14)	2.324(6)
Ru(2)–C(14)	2.218(5)	Ru(3)–C(13)	2.386(4)
Ru(4)–C(13)	2.149(5)	C(13)–C(14)	1.411(7)
C(12)–C(13)	1.501(9)	C(15)–C(16)	1.176(10)
C(14)–C(15)	1.441(8)	C(16)–C(17)	1.469(15)
Ru(2)–Ru(1)–Ru(4)	94.7(1)	Ru(1)–Ru(2)–Ru(3)	84.7(1)
Ru(2)–Ru(3)–Ru(4)	94.2(1)	Ru(1)–Ru(4)–Ru(3)	81.9(1)
Ru(1)–P(1)–Ru(3)	100.4(1)	Ru(1)–P(1)–Ru(2)	71.8(1)
Ru(2)–P(1)–Ru(4)	121.3(1)	Ru(1)–P(1)–Ru(4)	72.2(1)
Ru(2)–P(1)–Ru(3)	69.0(1)	Ru(3)–P(1)–Ru(4)	73.9(1)
C(12)–C(13)–C(14)	116.4(5)	C(13)–C(14)–C(15)	118.9(5)

via two σ-interactions to Ru(2) and Ru(4) [for **3a**: Ru(2)–C(13) = 2.176(3) Å, Ru(4)–C(14) = 2.139(4) Å; for **3c**: Ru(2)–C(14) = 2.218(5) Å, Ru(4)–C(13) = 2.149(5) Å] and η^2-bound to Ru(1) and Ru(3) [for **3a**, Ru(1)–C(13) = 2.393(3) Å, Ru(1)–C(14) = 2.494(3) Å, Ru(3)–C(13) = 2.361(4) Å, Ru(3)–C(14) = 2.384(3) Å; for **3c**, Ru(1)–C(13) = 2.361(4) Å, Ru(3)–C(14) = 2.324(6) Å, Ru(3)–C(13) = 2.386(4) Å, Ru(3)–C(14) = 2.369(4) Å]. The carbon atoms associated with these short σ-Ru–C bonds correspond to those of the longer Ru–C η^2-interactions. The reverse is true of the longer σ-Ru–C bonds. Such distortions are common in alkyne-containing clusters, not always due to asymmetry of the alkyne.[47] The C–C bond lengths of the pendant acetylenic ligands in these two clusters are comparable [C(15)–C(16) = 1.189(5) and 1.176(5) Å for **3a** and **3c**, respectively] and within the range expected for uncoordinated triple bonds.[40]

The presence of bridging and semibridging carbonyl ligands in the ground-state structures of **3a** and **3c** manifests itself in the ^{13}CO NMR spectra of these clusters. The room-temperature $^{13}C\{^1H\}$ NMR spectra of both **3a** and **3c** consist of one doublet resonance in the carbonyl region (δ = 200.8, $^2J_{PC}$ = 12.6 Hz **3a**, δ = 201.6, $^2J_{PC}$ = 11.1 Hz **3c**) associated with rapid exchange of all eleven carbonyl ligands on the NMR timescale. The $^{13}C\{^1H\}$ NMR spectrum in the carbonyl region of **3a** or **3c** exhibited a single broad doublet resonance even at the lowest temperatures accessible in the solvent of choice (−90 °C, CD_2Cl_2) implying an exceptionally low barrier to carbonyl scrambling. From an examination of the structures of **3a** and **3c** only two of the eleven carbonyl ligands present lie in the approximately square plane of metal atoms, those that bridge the Ru–Ru vectors C(11)–O(11) and C(12)–O(12). The remaining CO groups have character intermediate between pure axial and pure equatorial positions. Unfortunately, we have been unable to obtain a slow exchange spectrum precluding further examination of the mechanistic details of this remarkably facile exchange process, although a favorable pathway involves the delocalized exchange of all CO ligands about the Ru_4 plane facilitated by carbonyl bridge opening, trigonal rotation, and bridge closure along a different Ru–Ru bond. This process would require M–M bond elongation and contraction in a "breathing motion" Support for this arises from an examination of the ground-state structures of **3a**

Scheme II

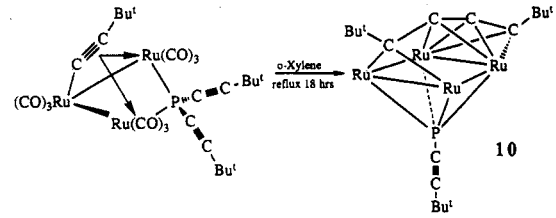

10

and **3c**. The two Ru–Ru bonds of intermediate length in **3c** [Ru(1)–Ru(2) = 2.807(1) Å, Ru(1)–Ru(4) = 2.807(1) Å] can be considered as one elongated "shortened" M–M bond and one shortened "normal" M–M bond lending support to the above proposal. Similar facile CO exchange processes at M_4 cluster square faces have been reported, notably in the related unsaturated clusters *closo*-$M_4(CO)_{10}(\mu\text{-}CO)(\mu_4\text{-}PPh)_2$ (M = Fe[44], Ru[45]), the benzyne, phosphinidene-capped cluster $Ru_4(CO)_{10}(\mu\text{-}CO)(\mu_4\text{-}PPh)(\mu_4\text{-}\eta^2\text{-}C_6H_4)$ [doublet carbonyl resonance δ 200; $^2J_{PC}$ = 12 Hz],[35b] and more recently the bis-sulfido-capped cluster $Ru_4(\mu_4\text{-}S)_2(CO)_7(\mu\text{-}CO)_2[C(NMe_2)_2]_2$.[48] The $^{13}C\{^1H\}$ NMR spectrum of the cluster $Ru_4(CO)_{10}(\mu\text{-}CO)(\mu_4\text{-}PPh)_2$ in the carbonyl region exhibited a single triplet resonance, there being no measurable effect upon lowering the temperature to −114 °C. The mechanism proposed for this facile exchange involved the intertransformation of carbonyl groups between the bridging and semibridging coordination modes coupled with an exchange of the out of plane (pseudoequatorial) terminal and the in-plane semibridging carbonyl ligands via the familiar merry-go-round mechanism.[45] Finally, analysis of the ^{13}C NMR spectrum of $Ru_5(CO)_{15}(\mu_4\text{-}PPh)$[49] revealed a rapid exchange process equilibrating all carbonyl ligands at room temperature. This exchange was partially frozen out at very low temperature (−95 °C), the NMR spectrum showing the apical carbonyl groups to be distinct from those of the square plane, the latter remaining in rapid exchange at this temperature. The dynamic behavior of this cluster bears a strong resemblance to that observed for the clusters **3a** and **3c** as well as **4a–b** (vide infra).

Transformation of 3a and 3b to 4a and 4b. Heating a toluene solution of **3a** (110 °C, 7–8 h) or an n-heptane solution of **3b** (97 °C, 3–4 h) resulted in a smooth conversion to $Ru_4(CO)_{10}(\mu_4\text{-}PPh)(\mu_4\text{-}\eta^1,\eta^1,\eta^3,\eta^3\text{-}RC_4R)$ (R = Ph, **4a**; R = $SiMe_3$, **4b**) in high yields. IR spectroscopic examination of these two products showed the absence of low-frequency bands due to μ_2-CO ligands. In the $^{31}P\{^1H\}$ NMR spectra a major shift of the phosphinidene signal (δ = 450 ppm, $\Delta\delta(^{31}P)$ = 200 ppm) to low field occurred. ^{31}P resonances in this region of the spectrum can be attributed to μ_4-PPh fragments coordinated on an electron-precise Ru_4 square face.[37] IR and ^{31}P NMR spectroscopic features suggested a structural assignment analogous to that of $Ru_4(CO)_{10}(\mu_4\text{-}PC{\equiv}C^tBu)(\mu_4\text{-}\eta^1,\eta^1,\eta^3,\eta^3\text{-}^tBuC_4{}^tBu)$ (**10**) recently prepared in our laboratories from $Ru_3(CO)_9(\mu_3\text{-}\eta^1,\eta^2,\eta^2\text{-}C{\equiv}C^tBu)[\mu\text{-}P(C{\equiv}C^tBu)_2]$[24] as shown in Scheme II.

A single-crystal X-ray analysis of **4b** (Figure 4) established the exact nature of the bonding of the hydrocarbyl fragment to the cluster framework. Final atomic positional parameters are listed in Table VIII, and Table IX contains an appropriate selection of interactomic bond distances

(47) Aime, S.; Osella, D.; Deeming, A. J.; Arce, A. J.; Hursthouse, M. B.; Dawes, H. M. *J. Chem. Soc., Dalton Trans.* **1986**, 1459.

(48) Bodensieck, U.; Stoecki-Evans, H.; Süss-Fink, G. *J. Organomet. Chem.* **1992**, *433*, 149.

(49) Natarajan, K.; Zsolnai, L.; Huttner, G. *J. Organomet. Chem.* **1981**, *209*, 85.

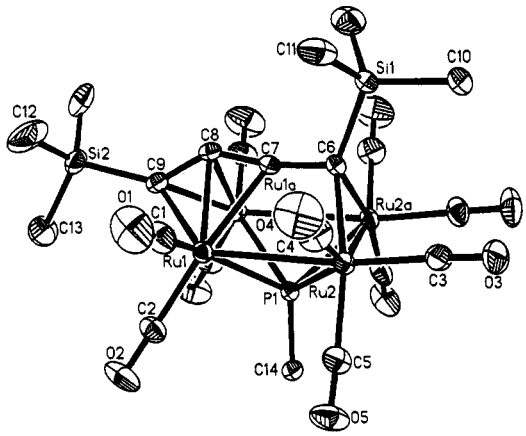

Figure 4. Perspective view of the molecular structure of $Ru_4(CO)_{10}(\mu_4\text{-}PPh)(\mu_4\text{-}\eta^1,\eta^1,\eta^3,\eta^3\text{-}SiMe_3C_4SiMe_3)$ (**4b**) (phenyl ring omitted for clarity).

Table VIII. Atomic Coordinates ($\times 10^4$) and Equivalent Isotropic Displacement Coefficients ($Å^2 \times 10^3$) for $Ru_4(CO)_{10}(\mu_4\text{-}PPh)(\mu_4\text{-}\eta^1,\eta^1,\eta^3,\eta^3\text{-}SiMe_3C_4SiMe_3)$ (4b)

	x	y	z	U(eq)[a]
Ru(1)	1274.8(1)	1539.1(2)	1837.1(2)	31.11(8)
Ru(2)	2193.4(1)	1479.3(2)	3737.0(2)	33.37(8)
P(1)	2159.5(5)	2500	2048(1)	28.2(3)
Si(1)	1114.5(7)	2500	5860(1)	40.2(5)
Si(2)	-165.9(7)	2500	621(2)	60.3(6)
O(1)	666(2)	-387(3)	2317(4)	105(2)
O(2)	1634(2)	718(2)	-492(3)	81(1)
O(3)	2990(2)	1366(3)	5901(3)	87(2)
O(4)	1489(2)	-259(3)	4570(4)	102(2)
O(5)	3064(2)	239(2)	2258(3)	78(1)
C(1)	894(2)	339(3)	2158(4)	60(2)
C(2)	1506(2)	1035(3)	395(3)	48(1)
C(3)	2689(2)	1448(3)	5106(4)	55(1)
C(4)	1748(2)	384(3)	4241(4)	61(2)
C(5)	2758(2)	710(3)	2820(3)	51(1)
C(6)	1515(2)	2500	4410(4)	30(1)
C(7)	1100(2)	2500	3462(4)	31(1)
C(8)	629(2)	2500	2777(4)	35(1)
C(9)	522(2)	2500	1576(4)	40(2)
C(10)	1664(3)	2500	7102(5)	62(2)
C(11)	607(3)	1412(4)	5953(5)	76(2)
C(12)	-613(3)	1406(5)	944(6)	104(3)
C(13)	114(4)	2500	-901(5)	96(4)
C(14)	2781(2)	2500	997(4)	34(1)
C(15)	2663(3)	2500	-201(5)	43(2)
C(16)	3164(3)	2500	-980(5)	55(2)
C(17)	3756(3)	2500	-569(6)	62(2)
C(18)	3871(3)	2500	606(6)	58(2)
C(19)	3386(2)	2500	1385(5)	44(2)

[a] Equivalent isotropic U defined as one-third of the trace of the orthogonalized U_{ij} tensor.

Table IX. Selected Interatomic Bond Distances (Å) and Angles (deg) for $Ru_4(CO)_{10}(\mu_4\text{-}PPh)(\mu_4\text{-}\eta^1,\eta^1,\eta^3,\eta^3\text{-}SiMe_3C_4SiMe_3)$ (4b)

Ru(1)–Ru(2)	2.955(1)	Ru(1)–Ru(1a)	2.682(1)
Ru(2)–Ru(2a)	2.849(1)	Ru(1)–P(1)	2.356(1)
Ru(2)–P(1)	2.404(1)	Ru(1)–C(7)	2.326(4)
Ru(1)–C(8)	2.219(4)	Ru(1)–C(9)	2.135(4)
Ru(2)–C(6)	2.190(3)	C(6)–C(7)	1.411(6)
C(7)–C(8)	1.290(7)	C(8)–C(9)	1.396(7)
Ru(2)–Ru(1)–Ru(1a)	91.6(1)	Ru(1)–Ru(2)–Ru(2a)	88.4(1)
Si(1)–C(6)–C(7)	112.7(3)	Si(2)–C(9)–C(8)	135.8(4)
C(6)–C(7)–C(8)	167.2(5)	C(7)–C(8)–C(9)	137.1(5)

and angles. The molecule has a crystallographic mirror plane containing both silicon atoms and the four acetylenic carbon atoms C(6), C(7), C(8), C(9) of the hydrocarbyl backbone. A severely distorted square planar arrangement of metal atoms is capped on one side by a μ_4-PPh group and on the other by an 8-electron donor C_4 hydrocarbon backbone of a 1,3-diyne ligand. There are three independent Ru–Ru bonds, one of these [Ru(1)–Ru(2)] and its symmetry-related bond are elongated [Ru(1)–Ru(2) = 2.955(1) Å]. Of the two remaining independent Ru–Ru bonds connecting the symmetry-related metals one bond is of normal length [Ru(2)–Ru(2a) = 2.849(1) Å] and the other is significantly shortened [Ru(1)–Ru(1a) = 2.682(1) Å]. This latter is bridged by three of the four carbon atoms of the 1,3 diyne ligand [Ru(1)–C(9) = 2.135(4) Å, Ru(1)–C(8) = 2.219(4) Å, Ru(1)–C(7) = 2.326(4) Å] while the opposite Ru–Ru edge is bridged in μ_3-alkylidyne fashion by the remaining carbon atom, C(6) [Ru(2)–C(6) = 2.190(3) Å]. We have previously observed a similar μ_4-C_4 hydrocarbon fragment prepared by the tail to tail coupling of two acetylides derived from a tris(*tert*-butylalkynyl)phosphine.[24] To our knowledge this represents the first example of the coordination of both triple bonds of a 1,3-diyne fragment to a single square face of a metal cluster. The four-carbon fragment of cluster **4b** has a different origin arising from the stepwise incorporation of one triple bond into cluster **1** via P–C coupling and then coordination of the second triple bond via the intermediacy of an electronically unsaturated cluster. This intermediate is expected to facilitate coordination of the second free acetylene donating a further four electrons. Scheme III illustrates this remarkable skeletal transformation (**1**–**4**). Although the origin of these two hydrocarbyl fragments in **4b** and **10** is different, they are structurally similar and we can describe the bonding of the diyne fragment to the Ru_4 square face as a bis(alkylidyne) dicarbide with each of the terminal [C(9)Si(2)Me_3; C(6)-Si(1)Me_3] fragments bonded to two metal atoms [Ru(1)–Ru(1a) for C(9); Ru(2)–Ru(2a) for C(6)] and a carbide-like carbon atom [C(8) or C(7)] in μ_3-fashion. The C(7)–C(8) distance is short [1.290(7) Å], and both C(8)–C(9) [1.396(7) Å] and C(6)–C(7), [1.411(6) Å] are elongated, consistent with an extensive rehydridization of the carbon atoms to fulfill the bonding requirements. The attachment of the C_2 unit [C(7)–C(8)] to the "boatlike" framework of Ru(1)–Ru(4), C(6), and C(9) has features in common with

Scheme III

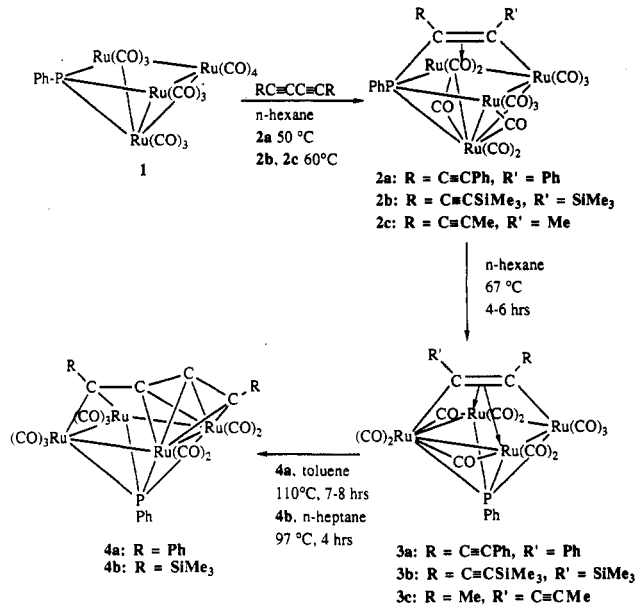

the coordination of the dicarbide unit in the Co_6 cluster $Co_6(\mu_6\text{-}C_2)(\mu\text{-}CO)_6(CO)_8(\mu_4\text{-}S)$.[50]

Few clusters have been prepared that incorporate both triple bonds of a 1,3-diyne ligand into a cluster face. The remarkably facile transformation reported here represents the first stepwise incorporation of two acetylenic multiple bonds. In contrast, Deeming has demonstrated that coordinative and electronic unsaturation in clusters containing a singly bound 1,3-diyne is compensated for by C(sp)–C(sp) cleavage to form bisacetylide clusters.[51] We found no evidence for such a process under the mild conditions employed here.

All attempts to prepare the analogous cluster $Ru_4(CO)_{10}(\mu_4\text{-PPh})(\mu_4\text{-}\eta^1,\eta^1,\eta^3,\eta^3\text{-}MeC_4Me)$ via a similar procedure to that employed for **4a** and **4b** proved unsuccessful. There was no evidence for the formation of this structural analogue, possibly due to the presence of hydrogen atoms bound to the α-carbons of the 1,3-diyne. Competing processes may include metallation (formation of allenyl type clusters) and C–C cleavage or fragmentation/condensation reactions.

The sequence outlined in Scheme III of **1** or **2a–c** to **3a–c** bears a strong resemblance to the coupling/decoupling reactions of acetylenes and a bridging sulfido group on the cluster $Os_4(CO)_{12}(\mu_3\text{-S})$, previously reported by Adams and Wang.[14b]

Hydrogenation of *nido*-$Ru_4(CO)_{10}(\mu\text{-}CO)_2\{\mu_4\text{-}\eta^1,\eta^1,\eta^2\text{-}P(Ph)C(C{\equiv}CPh)CPh\}$ (2a). Heating an n-heptane solution of cluster **2a** at 80–90 °C under a purge of dihydrogen led to a clean conversion to the known cluster $H_2Ru_4(CO)_{12}(\mu_3\text{-PPh})$[12] (**5**) liberating the corresponding monoene. Four

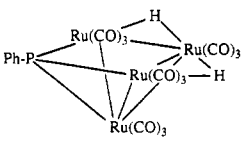

5

mole equiv of dihydrogen are consumed, three by the diyne and the remaining one in the generation of the dihydride. The organic byproduct was purified and the formulation established using GC–MS (parent molecular ion). The stereochemistry of monoene formation was established using ^1H NMR spectroscopy. The monoene product is *trans*-1,4-diphenylbut-1-ene, a fact confirmed by comparing its ^1H NMR spectrum with one previously reported.[52] With the ultimate objective of exploring the potential of **1** for the stoichiometric or catalytic reduction of diynes by H_2 we made a preliminary investigation of the conversion of $H_2Ru_4(CO)_{12}(\mu_3\text{-PPh})$ to **1** by CO in the presence of a hydrogen acceptor. Coordination of the 1,3-diyne occurs under mild conditions although hydrogenation is effected only at 90 °C. Elimination of the olefin presumably reflects the weakness of the attachment of the reduced substrate to the Ru_3P face. Remarkably, this coordination, hydrogenation, and elimination of the monoene occurs with retention of the cluster geometry; i.e., the phosphinidene remains in the basal plane (eqs 1–3). This contrasts with the relative ease of skeletal transformation (**2** to **3**) under thermal conditions in the absence of hydrogen.

$$\underset{\mathbf{1}}{Ru_4(CO)_{13}(\mu_3\text{-PPh})} + PhC{\equiv}CC{\equiv}Ph \xrightarrow{50\,^\circ C} \underset{\mathbf{2a}}{Ru_4(CO)_{10}(\mu\text{-}CO)_2[\mu_4\text{-}\eta^1,\eta^1,\eta^2\text{-}P(Ph)C(C{\equiv}CPh)CPh]} \quad (1)$$

$$\underset{\mathbf{2a}}{Ru_4(CO)_{10}(\mu\text{-}CO)_2[\mu_4\text{-}\eta^1,\eta^1,\eta^2\text{-}P(Ph)C(C{\equiv}CPh)CPh]} \xrightarrow[H_2]{90\,^\circ C} \underset{\mathbf{5}}{H_2Ru_4(CO)_{12}(\mu_3\text{-PPh})} + trans\text{-}PhCH_2CH_2CH{=}CHPh \quad (2)$$

$$\underset{\mathbf{5}}{H_2Ru_4(CO)_{12}(\mu_3\text{-PPh})} \xrightarrow[UV]{C_6H_{10},\,CO} \underset{\mathbf{1}}{Ru_4(CO)_{13}(\mu_3\text{-PPh})} \quad (3)$$

Hydrogenation and elimination of coordinated hydrocarbyl fragments have previously been described,[51] and most recently the hydrogenation of the organic fragment (a β-metallated monoazadien-4-yl (MAD-yl) [$R^1C{=}CH\text{-}CH{=}NR^2$]) coordinated to a linear Ru_4 cluster has been described affording $H_4Ru_4(CO)_{12}$ via elimination of the free volatile organic secondary amine $R^1CH_2CH_2\text{-}CH_2NR^2H$.[53] Several phosphinidene-stabilized clusters, including **1**, have recently been examined as potantial homogenous hydrogenation/isomerization catalysts.[54] While the iron derivatives (including $Fe_3(CO)_9(\mu\text{-}CO)(\mu_3\text{-PR})$ (R = ^{i}Pr, $PNEt_2$), $(\mu\text{-H})Fe_3(CO)_9(\mu_3\text{-}PC_6H_4OMe)$) showed only moderate activity, cluster **1** was considerably more active in both processes, the outcome depending largely on the reaction time and temperature. The ease with which **2a** reacts with dihydrogen supports the proposal that μ-PPh-containing clusters which have undergone insertion of alkynes into M–P bonds are intermediates. These readily release the alkene. We found no evidence (under similar conditions to those used for the hydrogenation) for the elimination of an alkene from **3a–c** suggesting that over prolonged catalytic reaction times formation of this more stable cluster is responsible for the catalytic deactivation and loss of activity.

Conclusion

In summary, we have demonstrated that cluster **1** represents a viable high-yield route to alkyne-containing clusters, addition first occurring in a highly regiospecific manner with P–C bond formation to afford a cluster-bound alkyne coordinated in the familiar $2\sigma\text{–}\pi$ fashion. This mode of coordination is unusual occurring at the open Ru_2P triangle of an Ru_3P square face of a square pyramidal framework, further reinforcing the proposal that a μ_3-PPh fragment can act as an integral part of the skeletal framework. Decarbonylation of such clusters initiates a "skeletal isomerization" in which the basal μ_3-PPh vertex of the square pyramid migrates to the apical position to adopt its more familiar role as a μ_4-PPh cluster stabilizing fragment. This facile Ru_4P framework rearrangement makes cluster **1** a particularly attractive model for surface processes. The square Ru_3P face of the square pyramidal

(50) Gervasio, G.; Rossetti, R.; Stanghellini, P. L.; Bor, G. *Inorg. Chem.* **1984**, *23*, 2073.
(51) Deeming, A. J.; Felix, M. S. B.; Bates, P. A.; Hursthouse, M. B. *J. Chem. Soc., Chem. Commun.* **1987**, 461.
(52) Snider, B. B.; Jackson, A. C. *J. Org. Chem.* **1983**, *48*, 1471.
(53) (a) Mul, W. P.; Elsevier, C. J.; Leijen, M. V.; Vrieze, K.; Smeets, W. J. J.; Spek, A. L. *Organometallics* **1992**, *11*, 1877. (b) Mul, W. P.; Elsevier, C. J.; Vrieze, K.; Smeets, W. J. J.; Spek, A. L. *Organometallics* **1992**, *11*, 1891.
(54) Castiglioni, M.; Giordano, R.; Sappa, E. *J. Organomet. Chem.* **1991**, *407*, 377.

skeleton presents an opportunity to evaluate chemistry at a mixed main group–transition metal surface while the square Ru_4 fragment generated by the rearrangement process is attractive as a model for a ruthenium (100) surface.

The diyne ligands bound to the square Ru_4 face in the transformed clusters have the now familiar μ_4–η^2 coordination mode. In each case the presence of a pendant unsaturated unit offers the opportunity for further transformations either through C–C bond cleavage, incorporation of the alkyne into the skeletal framework or via cluster linking. Clusters **3a,b** undergo a more remarkable transformation retaining the basic square pyramidal Ru_4P skeleton while incorporating the pendant triple bond of the coordinated 1,3-diyne. This represents the first such example of a quantitative stepwise addition and ligation of both triple bonds of a 1,3-diyne ligand to a cluster framework. We have successfully hydrogenated and eliminated the organic functionality from cluster **2a** and identified the organic byproduct as the trans monoene. As a result of these studies we believe that clusters **3a–c** represent potential precursors to the class of μ_4-PPh monocapped square planar M_4 clusters which have so far eluded synthesis. Theoretical studies by Hoffmann and co-workers have predicted that such molecules should be stable.[42a] We are presently pursuing alkyne elimination from the clusters *closo*-**3a–c**, having already undergone the "skeletal isomerisation" required for the formation of these elusive Ru_4P frameworks.

Acknowledgment. We are grateful to the Natural Sciences and Engineering Research Council of Canada for financial support of this work in the form of operating and equipment grants (to A.J.C.) and a scholarship (to J.F.C.).

Supplementary Material Available: Structural analyses, anisotropic thermal coefficients (Tables S1, S5, S8, and S12), remaining bond distances and angles (Tables S2, S6, S9, and S13) and hydrogen atom coordinates (Tables S3, S7, S10, and S14) for **2c**, **3a**, **3c**, and **4b** (19 pages). Ordering information is given on any current masthead page. Structure factors (Tables S4 (**2c**), S11 (**3c**), and S15 (**4a**)) are available upon request from the authors.

OM920557Q